ChemPlusChem

Review
doi.org/10.1002/cplu.202300214

Chemistry
Europe
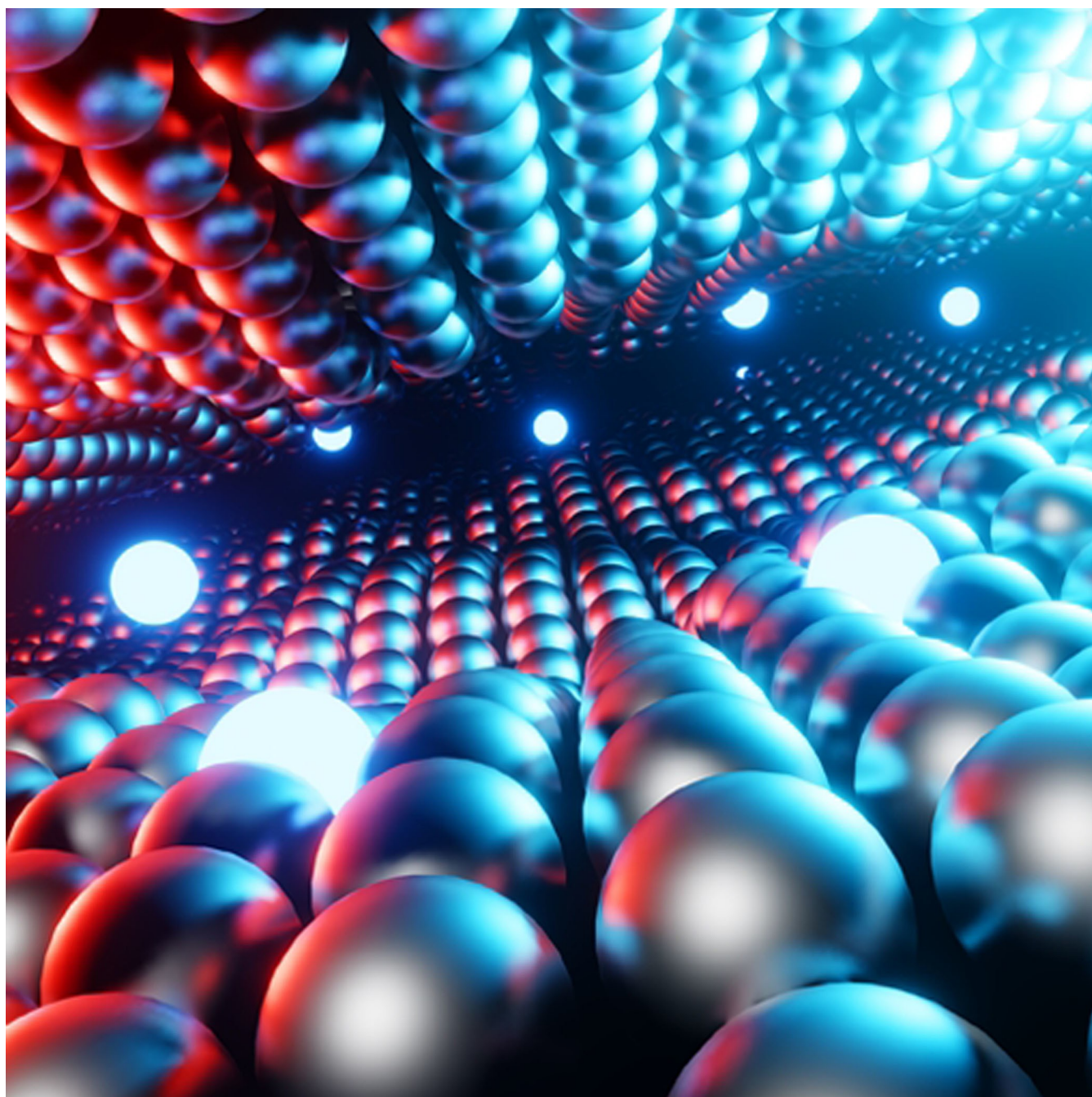European Chemical
Societies Publishing

www.chempluschem.org

Extending the Chemistry of Layered Solids and Nanosheets: Chemistry and Structure of MAX Phases, MAB Phases and MXenes

Niels Kubitza,[a] Carina Büchner,[a] Jordan Sinclair,[b] Rose M. Snyder,[b] and Christina S. Birkel*[a, b]

ChemPlusChem

Review

doi.org/10.1002/cplu.202300214

Chemistry Europe
European Chemical
Societies Publishing

MAX phases are layered solids with unique properties combining characteristics of ceramics and metals. MXenes are their two-dimensional siblings that can be synthesized as van der Waals-stacked and multi-/single-layer nanosheets, which possess chemical and physical properties that make them interesting for a plethora of applications. Both families of materials are highly versatile in terms of their chemical composition and theoretical studies suggest that many more members are stable and can be synthesized. This is very intriguing because new combinations of elements, and potentially new structures, can lead to further (tunable) properties. In this review, we focus on the synthesis science (including non-conventional approaches) and structure of members less investigated, namely compounds with more exotic M-, A-, and X-elements, for example nitrides and (carbo)nitrides, and the related family of MAB phases.

1. Introduction

MAX phases and their two-dimensional siblings, MXenes, are large – and continuously growing – families of materials that not only attract interest because of their (potential) applications but also for fundamental challenges related to their synthesis, structure, and chemistry. Many elements form MAX phases and can be exfoliated into MXenes (see Figure 1). The reader is also referred to books that cover many aspects of the respective materials[1,2] as well as the most recent review article that lists all known MAX phase compositions.[3]

MAX phases are ternary transition metal-based carbides, nitrides and carbonitrides that crystallize in a layered structure, typically in the hexagonal space group $P6_3/mmc$, but other structures are reported as well (see Section 3). They contain M_6X octahedra (M are early-to-mid transition metals, X is C and/or N or in rare cases it can be boron or selenium in combination with boron), a structural motif that is found in binary carbides, such as TiC, ZrC, and VC (basically the NaCl crystal structure). These edge-sharing octahedral layers are interleaved with layers of the A-element (main group elements in groups 13–16 and/or late transition metals). Depending on the number of octahedral layers along the c-axis sandwiched in between the A-layers, they are categorized as "211", "312", "413", and so on MAX phases. The general formula is $M_{n+1}AX_n$ with $n=1$, 2, 3 etc. for 1, 2, 3 etc. octahedral layer/s, respectively (see Figure 2). Electronically, MAX phases exhibit covalent (strong M–X bonds), ionic (relatively weak M–A bonds) and metallic (density of states at the Fermi Energy dominated by the d-orbitals of the M-atoms) contributions. This gives rise to two important characteristics: MAX phases behave like metals, they are electronically and thermally conductive, and, in some cases, the A-element (mostly aluminum), which is bonded more weakly, can be

chemically removed. The latter leads to van der Waals-stacked M–X nanosheets (MXenes).

MXene nanosheets are therefore transition metal-based carbides and (carbo)nitrides comprised of the metal-carbon/nitrogen octahedra that remain from the precursor MAX phases. As a result of their synthesis with hydrofluoric/hydrochloric acid as etchants, they also possess stabilizing surface functional groups, mostly –F, –Cl and –OH (denoted as T_x in the general MXene formula $M_{n+1}X_nT_x$). Consequentially, their surface chemistry is highly variable through different processing, e.g., washing, vacuum treatment and annealing, or through attachment of molecules onto the surface. Small molecules are typically used to intercalate in between the MXene sheets to delaminate the van der Waals-stacked sheets into few-layer or single sheets. The two-dimensional carbide/nitride flakes can be vacuum filtered into films that are metallic or can be handled as stable colloidal solutions. Please note that some MXenes are prone to oxidation and need to be stored under inert conditions.

The structural and functional properties of the layered MAX phases as well as the low-dimensional MXenes have been summarized and discussed in detail over the last one to two decades. The reader is referred to some excellent (review) articles[4–14] and books/book chapters.[1,15] This review focuses on the chemistry and synthesis science related to MAX phases and MXenes. More specifically, variations of and alternatives to the most discussed members of the two families will be summarized. The majority of published works deal with Ti-based members of MAX phases and MXenes. However, it is noted that more than 150 MAX phases (full MAX phases and solid solutions) are known, and many more chemical compositions have been theoretically predicted to form stable MAX phase structures. Therefore, MAX phases and MXenes beyond Ti as the M-element are worth a special focus review. Aside from the M-

[a] N. Kubitza, Dr. C. Büchner, Prof. Dr. C. S. Birkel
Department of Chemistry and Biochemistry
Technische Universitaet Darmstadt
64287 Darmstadt (Germany)
E-mail: christina.birkel@asu.edu

[b] J. Sinclair, R. M. Snyder, Prof. Dr. C. S. Birkel
School of Molecular Sciences
Arizona State University
Tempe, AZ 85281 (USA)
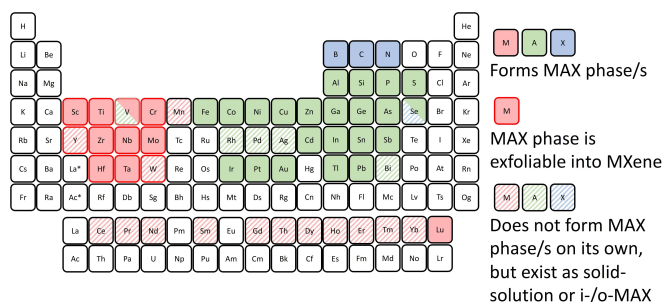
Figure 1. Periodic table marking all elements that form MAX phases and MXenes.

ChemPlusChem

Review
doi.org/10.1002/cplu.202300214

Chemistry Europe
European Chemical
Societies Publishing

MAX

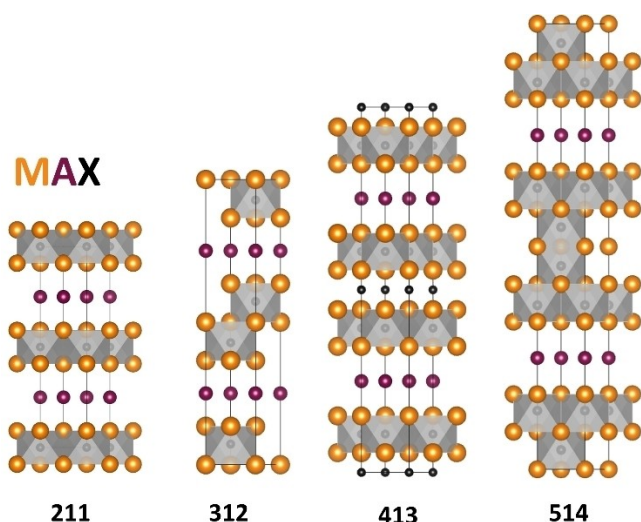211   312   413   514

Figure 2. Structures of MAX phases for $n = 1–4$.

and the A-elements, MAX phases and MXenes "beyond carbon" are also significantly less discussed in the literature and will be

an additional point of focus for this article. These topics will be connected through the following structure:

After briefly summarizing the history (Section 2) and structure of MAX phases and MXenes (Section 3), we will discuss variation of the M- (Section 4), A- (Section 5) and X- (Section 6) elements separately. We will then provide an extensive overview of synthesis strategies (Section 7) to prepare MAX phases and MXenes, particularly highlighting non-conventional and less-studied approaches before concluding with some summarizing and forward-looking remarks (Section 8).

2. Brief history of MAX phases and MXenes

2.1. MAX phases

The first synthesis of a member of the MAX phase family was reported by Kudielka and Rhode in 1960. They prepared two carbosulfides, Ti_2SC and Zr_2SC, in the form of single crystals and powders and showed that they crystallize in space group $P6_3/mmc$.[16] However, the name "MAX phase" did not exist until more than 30 years later (refer to Barsoum $et\ al.$'s work below). Nowotny $et\ al.$ summarized this group of hexagonal complex

Niels Kubitza is a PhD candidate at the Technische Universität Darmstadt (GER) in the Lab group of Christina Birkel. He joined the group in 2018 for his bachelor studies and went on by completing his master's thesis at the Arizona State University (USA) as a research scholar in 2020. In his research, Niels is focusing on the non-conventional synthesis of MAX phase nitrides and carbonitrides, as well as the synthesis of magnetic interesting antiperovskite phases.

Carina Büchner is a Postdoc in the Group of Prof. Christina Birkel since 2022. She conducts her Postdoc at Technical University of Darmstadt including a research stay at the Arizona State University. Her research focuses on the synthesis of carbide-based MAX phases, MAX like phases and MXenes. After completing her Masters of Science in chemistry at the Technical University of Darmstadt, she completed her PhD in 2022 in the same university. Her PhD research focused on the investigation of transition metal borides towards their electrocatalytic properties in the Group of Prof. Barbara Albert.

Jordan Sinclair is a PhD student at Arizona State University (ASU) in the group of Christina Birkel. He joined the group in 2021 after completing his Bachelors of Science (B.S.) at the University of Delaware and conducting solid state chemistry research under Professor Svilen Bobev. Currently, Jordan is mainly studying sol-gel synthesis of exotic MAX phase carbides and nitrides and is working to develop new synthesis strategies beyond conventional solid state methodologies.

Rose M. Snyder works as a Ph.D candidate with Dr. Christina Birkel at Arizona State University in Phoenix, Arizona. After completing her Bachelor of Science (B.S.) in Chemistry at Rowan University in 2016, she went on to work in industry as an inorganic chemist before taking a graduate research position in 2019. Her current research focuses on the synthesis and characterization of MAX phases and MXenes and their electrochemical applications.

Christina Birkel is an Associate Professor in the School of Molecular Sciences at Arizona State University and holds a joint professorship position in the Department of Chemistry and Biochemistry at the Technische Universität (TU) Darmstadt. Prior to her current positions, she was a Junior Research group leader at TU Darmstadt (Habilitation in 2018), a Postdoctoral Researcher (group of Prof. Galen Stucky) at the University of California, Santa Barbara (Feodor Lynen Research Stipend, Alexander-von-Humboldt Foundation) and completed her PhD thesis (group of Prof. Wolfgang Tremel) at the Johannes Gutenberg-University of Mainz holding a stipend of the MAINZ Graduate School of Excellence (2010).

ChemPlusChem

Review
doi.org/10.1002/cplu.202300214

Chemistry
Europe

European Chemical
Societies Publishing

carbides as "H-phases" or Cr_2AlC-type phases.[17] While "H-phases" exclusively encompass ternary carbides and nitrides with 211 stoichiometry, the authors noticed that Ti_3SiC_2-type compounds (later called 312 MAX phases) exhibit very similar structures with edge-sharing transition metal-carbon/nitrogen octahedra but larger c-lattice parameters. Note that "H-phases" are not a different name for Hägg carbides, which is sometimes falsely assumed in the literature. Nowotny and/or Jeitschko (who was one of Nowotny's PhD students) synthesized an impressive number of MAX phases in the 1960s including the 312 phases Ti_3SiC_2[18] and Ti_3GeC_2.[19] However, interest in these compounds, aside from their synthesis and structure, was very limited for the decades that followed. Ti_3SiC_2 may have been an exception as researchers started to investigate its properties, e.g., hardness and decomposition behavior, as early as 1972/73.[20,21] Some conflicting results relating to its temperature/oxidation stability occurred following these earlier reports. Above everything else, these debates show how crucial the quality of the MAX phase product is since the presence of side phases affects the properties tremendously.

Major breakthroughs in the field of MAX phases were triggered by the production of high-quality Ti_3SiC_2 by means of reactive hot pressing at 40 MPa and 1600 °C starting from TiH_2, SiC and graphite in 1996.[22] Turning their attention to some of the 211 phases, the researchers found very similar properties for Ti_2AlC, Ti_2AlN and Ti_2GeC.[23] This solidified their idea that they are dealing with a large family of layered solids. And it was about to grow further, when the team reinvestigated earlier reports on the synthesis of "Ti_3AlN_2" which they later showed to be Ti_4AlN_3 which has a larger c-lattice parameter (~23 Å) in comparison to 312 phases (~18 Å).[24] Reports on further 413 MAX phases followed adding Ta_4AlC_3,[25] V_4AlC_3[26] and Ti_4GaC_3[27] to the family which now consisted of a remarkable number of compounds, especially considering solid solution compounds. For detailed information on their structure as well as mechanical, chemical, and physical properties the reader is referred to the book "MAX phases" by Michel Barsoum.[1]

The MAX (and MXene) community received another boost when ordered MAX phases were discovered (in 2014 and 2017). In contrast to solid solution compounds with random distribution of the elements on the M- or A-site, so-called o- and i-MAX phases exhibit specific ordering of the M-element. This was first found for 312 MAX phases with a ratio of 2:1 for the M-elements translating into ordering of the three M-layers in the structure. For the first member, $(Cr_{2/3}Ti_{1/3})_3AlC_2$,[28] this leads to alternating layers consisting of either Cr or Ti only (Cr and Ti on the 4f and 2a Wykoff site, which are on the outer and inner layer/s, respectively). The compound still crystallizes in the space group typical for MAX phases, $P6_3/mmc$. A few years later, ordered 211 MAX phases were synthesized for the first time. The first example, $(Mo_{2/3}Sc_{1/3})_2AlC$,[29] exhibits in-plane ordering where the Sc atoms extend out of the Mo plane towards the Al atoms. This changes the crystal structure from hexagonal to monoclinic ($C/2c$). The discovery of both new versions of MAX phases was quickly followed by further theoretical and experimental work as well as exfoliation into new types of MXenes.[30] Most notably, these compounds enable incorporating elements

that typically do not form MAX phases as well as new chemical compositions and combinations. Pushing the chemical diversity of MAX phases (and MXenes) even further, MAX phases with several different elements on the M-site have been prepared that belong to the family of medium entropy alloys. For example, Nemani et al. demonstrated that four transition metals can share the M-position in equimolar proportions of Ti:V:Nb:Mo and Ti:V:Cr:Mo, respectively.[31]

While the previous stated milestones in the research of MAX phases were mostly based on forming new compounds using elemental reactants or suitable precursors, just recently, Huang et al. reported a revolutionary approach to use chemical scissors and intercalants to either replace A-elements in already known MAX phases by uncommon elements (e.g. iron, zinc) or to produce MXenes with regulated surface termination. This in turn leads to new potential applications (e.g. magnetism), combined with a large number of new members in the family of MAX phases.[32]

2.2. MXenes

In 2011, Naguib, Gogotsi, and Barsoum, at Drexel University, selectively removed Al from a MAX phase, Ti_3AlC_2, and produced $Ti_3C_2T_x$[33] for the first time; a 2D nanomaterial that was both strong and flexible. They named the new material MXene (pronounced MAXene), the 'MX' for the elements left after etching and the'ene' as a reference to graphene, one of the most popular 2D materials.

This initiated tremendous MXene research (some highlights are discussed in this section), which involved the wet etching of other MAX phases, including Ti_2AlC,[34] Ta_4AlC_3,[34] V_2AlC,[35] V_4AlC_3,[36] and so on. This technique is also employed for i-MAX phases (e.g., $Mo_{4/3}Y_{2/3}AlC$),[37] o-MAX phases (e.g., Mo_2TiAlC_2),[38] and solid solutions (e.g., $(Cr_{1-x}V_x)_2AlC$).[39] For reference, MXenes that have been synthesized to date are depicted in Figure 1. In 2019, the first MXene with 5 metal layers was synthesized via wet acid-etching, $Mo_4VC_4T_x$,[40] expanding the MXene family and furthering interest in higher order MXenes.

MAX phases are generally the primary precursor for MXene synthesis. However, some MAX phases are not thermodynamically stable and therefore are not available to produce their MXene counterparts. In 2015, the MAX-like phase, Mo_2Ga_2C, was selectively etched in hydrofluoric acid to produce Mo_2CT_x.[41,42] Other non-MAX phases (those with layered structures, but different ordering/space groups) have also been exfoliated. $Hf_3[Al(Si)]_4C_6$ has been etched to form $Hf_3C_2T_x$[43] and $Zr_3Al_3C_5$ has been etched to form $Zr_3C_2T_x$.[44]

In 2015, Xu et. al.[45] utilized chemical vapor deposition (CVD) to create Mo_2C thin films. They used methane and molybdenum foil to create nanometer thick films. It was found that by tuning the synthesis temperatures, the control of the lateral size of the flakes and thickness of the sheets is possible. Because of this, CVD is known for its ability to create scalable, uniform thin carbide films with less defects than MXenes produced by traditional acid-based etching.[45]

ChemPlusChem

Review
doi.org/10.1002/cplu.202300214

Chemistry Europe
European Chemical
Societies Publishing

Compared to carbides, nitride and carbonitride MXenes are somewhat rare, for a few reasons. Research into carbonitride and nitride MXenes is lagging, with fewer of their parent MAX phases available compared to their carbide counterparts (see Section 6). Additionally, due to the dissolution of the nitride layer in acidic media, careful consideration must be made into their synthetic conditions. Ti_3CNT_x carbonitrides were first synthesized in 2012 using traditional acid wet-etching.[34] In 2016, $Ti_4N_3T_x$ was synthesized using a molten fluoride salt mixture[46] and molten salt synthesis has continued to be a popular technique for etching other nitrides, such as Ti_2NT_x[47] and V_2NT_x.[48] Additionally, instead of selective removal of the A-layer in nitride MAX phases, element replacement of C with N in as-synthesized carbide MXenes via ammoniation was done in 2017 to create Mo_2NT_x and V_2NT_x.[49]

In 2017, MBenes, a sibling class to MXenes, were first predicted.[50] $Mo_{4/3}B_2$ is the only 2D MBene that has been synthesized.[51] While MBenes represent a large class of materials with varying layered structures, there are certain compositions that resemble MXenes (i.e. $M_{n+1}B_n$), and thus fall into that classification instead (now referred to as boron-containing MXenes).[52] It is predicted that Ti_2B,[53] Mo_2B,[54] and Hf_2B[55] are stable species.

The addition of boron-based MXenes, high entropy phases, and higher-order MXenes means that this class of roughly $40+$ synthesized materials (with over 100 possible compositions)[56] is growing rapidly. With changing elemental compositions, layer thickness, and polymorphs, there are endless possibilities for materials development due to their extensive flexibility in elemental compositions and tunability, their applications are wide, ranging from energy storage in batteries[30] to electromagnetic interference shielding[57] to biosensors.[58,59]

3. Structure of MAX phases and MXenes

3.1. 211, 312, 413, 514 MAX phases

MAX phases consist of at least three different elements (ternary nitrides, carbides, in rare cases borides or selenides). The M-element is a transition metal with a group number lower than seven or a rare earth metal in compounds with two different M-elements. The A-element is an element with a group number between twelve and sixteen or a transition metal with a group number of eight or higher. The X-element is carbon or nitrogen,[60] in rare cases it can also be boron or selenium.[55,61,62] Common MAX phases have a hexagonal symmetry with the space group $P6_3/mmc$ (#194). M- and X-elements form layers of edge-shared octahedra whereas the octahedra are centered by carbon and the M-elements occupy the octahedra edges. Strong covalent bonds are present between M- and X-atoms. These octahedral layers can exist as single layers or multi layers which are interconnected via shared edges. The M- and X-atom layers are separated by mostly single atomic A-element-layers with week bonds to the M-atoms. Thus, the sum formula of MAX phases is $M_{n+1}AX_n$ for a number of n layers.[60,63] To state the number of layers of a respective MAX phase the abbrevia-

tion "$n+1'1'n$" is commonly used. For example, a MAX phase with $n=2$ can be stated as 312. The highest value of n for a MAX phase which has been realized experimentally in a bulk compound to date is 4. Only two publications on MAX phases with $n=4$ exist. The structures of MAX phases with $n=1–4$ are displayed in Figure 2. One of them describes the recent discovery of Mo_4VAlC_4. The structure is not fully solved yet. Instead of typical stacking of octahedra facing towards the same direction, the direction in which the octahedra point changes in the center of the layers, which leads to a herringbone-type structure.[40] $(Ti_{0.5}Nb_{0.5})_5AlC_4$ in contrast has the typical MAX phase structure with all octahedra faced towards the same direction.[64] In most of the currently known MAX related phases only single atomic sheets of A-elements are located between the octahedral layers.[60] Mo_2Ga_2C and Nb_2Bi_2C[32] are the only experimentally available bulk phases which have a MAX phase-based structure but instead of single sheets of A-atom layers between the octahedral layers directly stacked double A-atom layers are present.[65–67] Mo_2Ga_2C exhibits the same symmetry as common MAX phases (space group $P6_3/mmc$, #194) and the same $M–X$ building units which are edge shared octahedrons. Instead of one A-element layer, two A-element layers with the A-atoms directly stacked on top of each other in the c-direction separate the $M–X$-layers. Therefore, in publications this phase is not considered to be a MAX phase and is usually described as a MAX phase related compound.[65,68] Furthermore, V_2Ga_2C in the same structure as Mo_2Ga_2C has been predicted to be stable.[67] $Ti_3Au_2C_2$ has been synthesized in form of thin films. In this compound the Au atoms in the double-A-layer are shifted towards each other and are not located on top of each other.[69] Other compounds with the sum formula M_2S_2C (S=sulfur) exist but don't have the MAX phase structure.[70] Besides these MAX phases with well-defined compositions, the number n of octahedral layers can vary within a substance from layer to layer. These phases are called intergrown MAX phases. Higher stacking numbers $n>4$ have been observed in HRTEM images for the Ta–Al–C ($n=5$)[60,63] and Ti–Sn–C ($n=6$)[71] intergrown system but only in a few unit cells of the samples.[60] Most of the time, n varies periodically only between two numbers. The sum formula of the particular MAX phase hence is stated as $M_{na+nb+2}A_2X_{na+nb}$, whereat na and nb are the different numbers of interconnected layers.[60]

3.2. Double-M ordered MAX phases

Aside from solid solutions, two different M-elements can occupy the metal sites in an ordered arrangement. The ordering can be present as out-of-plane ordering perpendicular to the M-layers, abbreviated as o-MAX phases, or the different elements can be ordered two-dimensionally in the direction of the M-layers, abbreviated as i-MAX phases.

For out-of-plane ordering the symmetry of the MAX phase is maintained. To enable out-of-plane ordering, n must be equal or higher than 2. Different Wyckoff positions for M-elements in 312 and 413 phases make this ordering possible without loss of the hexagonal symmetry.[72] The respective structures are shown

ChemPlusChem

Review

doi.org/10.1002/cplu.202300214

Chemistry
Europe
European Chemical
Societies Publishing

in Figure 3. Reports about *o*-MAX phases are limited. Previously synthesized *o*-MAX phases are aluminum carbides containing a mixture of earlier and later *M*-elements, namely chromium in combination with titanium[73,74] or vanadium[75] and molybdenum in combination with titanium[76,77] or scandium.[78] The existence of additional stable *o*-MAX phases has been predicted by Dahlqvist and Rosen.[72]

Between 2017 and 2019 a row of in-plane ordered MAX phases, *i*-MAX, have been found.[29,79–87] The in-plane ordering occurs in MAX phases with $n = 1$ (Figure 3). Two thirds of *M*-positions within the plane are occupied by the major element *M'* and one third by the minor element *M''*.[88] The in-plane ordering causes a symmetry reduction from hexagonal to monoclinic (*C2/c*, #15[29,80–82,84–87,89] or less common *C2/m*, #12[87]) or orthorhombic (*Cmcm*, #63)[79,80,82,83] symmetry. The distances from *M''*-elements to *A*-atoms are decreased compared to the *M'*-*A*-distances. This leads to the formation of a trigonal *M''*-sublattice and honeycomb-like *M'*-arrangement. The main reason for the ordering and the symmetry reduction is the difference of *M*-element radii whereas *M''* is the larger element.[79,85] The larger the *A*-element radius, the higher must be the difference of *M*-element radii to achieve the formation of an *i*-MAX phase.[88] Hence the formation of *i*-MAX phases is more favorable for smaller *A*-elements. This has been found by Dahlqvist and Rosen through calculations and is supported by the currently experimentally available MAX phases.[88] Reports about *i*-MAX phases include several uncommon *M*-elements, like rare earth metals, tungsten, and manganese. In most of the previously synthesized *i*-MAX phases the *A*-element is aluminum or gallium.[29,79–87] Plenty of further stable *i*-MAX phases have been predicted by Dahlqvist and Rosen recently.[88] Thore *et al.* conducted first principal calculations for double-*A*-element MAX phases with the sum formula (Mo,V)$_2$Ga$_2$C. Mo$_{1.5}$V$_{0.5}$Ga$_2$C is predicted to form an ordered MAX phase structure.[67]

3.3. MXenes

Following the exfoliation (etching with acid which removes the *A*-element, often Al) and delamination (intercalation of small molecules to separate the sheets), the MXene forms first as van der Waals-stacked multilayers and subsequently as few-layers and ultimately single-layer sheets. The MXene sheets adopt
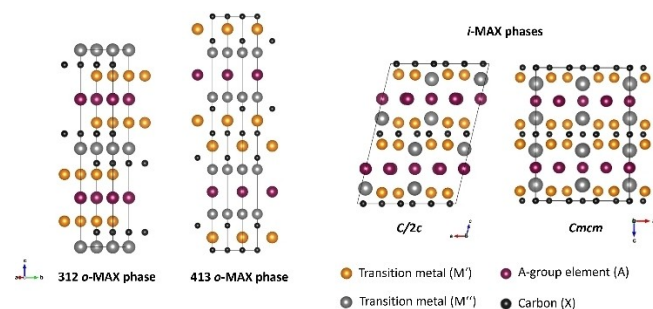
their parental MAX phase structure within the *M*–*X*-layers but the *A*-layers are not present anymore in a fully exfoliated MXene. That means they also consist of edge-shared octahedrons that can be stacked on top of each other in layers up to $n = 4$.[11,40] Ordered arrangements within the *M*–*X*-layers are maintained which is the case for MXenes from *o*-MAX or *i*-MAX phases.[40,74,77,78,84,89] Moreover, the etching of *i*-MAX phases can introduce in-plane ordered vacancies into the *M*–*X*-layers if the minor *M*-element is removed by the etchant without destroying the bonds of the major element and the *X*-atoms. This has been proven by the etching of rare earth metals from MAX phases by HF.[29,81,89]

Another factor to consider when describing the structure of MXenes is terminating surface functional groups and intercalating cations between the sheets. These species strongly depend on the exfoliation method, the delamination method, and further processing. After treatment with aqueous fluoride-based etchants (most common), the functional groups are −H, −OH, −F or −O. For titanium-based MXenes it has been found that −F and −O termination groups are most stable and −OH groups decompose to −O groups over time.[90–92] If chlorides are used during the etching process, these groups are found as well.[93] The surface groups which are present after the exfoliation can be further functionalized or modified.[94] The distance of the exfoliated layers changes depending on whether a multilayer MXene or a fully delaminated MXene is present and depends on the surface functionalization.

The most accessible way to determine that the final product is a MXene is X-ray diffraction, a technique that gives clear insights into the crystal structure at each step of the process. For a successful MAX phase to MXene conversion, the (00 *l*) reflections in the diffraction pattern show a shift to lower angles due to the unit cell expansion into the *z* direction from the exfoliation process. In multilayered MXene samples, this shift will not be as high as for the fully delaminated MXene film, as the van der Waals forces still hold the sheets more tightly together. This shift of the (00 *l*) peaks increases after the delamination process, due to intercalated water expanding the unit cell in the *z* direction and then full separation of lamellae. The X-ray diffraction pattern of a MXene-film shows a strong preferred orientation so that the (00 *l*) peaks show an increased intensity in the pattern. The (002) peak has the strongest intensity, which appears at a relatively low diffraction angle (between 3 and 15 °2θ). A well etched MXene will produce evenly spaced (00 *l*) peaks and a high intensity due to the high preferred orientation. Both structures can be additionally confirmed using electron microscopy (SEM), where the multilayered product will usually have an accordion-like structure and the delaminated product will show large, thin sheets.[95]

4. Variation of *M*

4.1. Most common *M*-elements

First investigations of *M*-site solid solution phases reach back to 1980s, when Schuster and Nowotny *et al.*[96–98] already reported

Figure 3. Structures of ordered double-*M* MAX phases for out-of-plane (*o*-MAX) and in-plane (*i*-MAX) ordering.

ChemPlusChem

Review
doi.org/10.1002/cplu.202300214

**Chemistry
Europe**
European Chemical
Societies Publishing

H-phases that exhibit solubility on the M-site. Here, the choice of M-elements was restricted to the groups 4, 5, and 6 and combinations of Ti–Nb, V–Nb, V–Cr, V–Ti, Cr–Ti, and Ti–Ta were tested. All phases, except for the $(Cr_{1-x}Ti_x)_2AlC$[97] solid solution exhibit complete miscibility on the M-site by maintaining the $P6_3/mmc$ structure. Roughly 20 years later, first property measurements of solid solution phases were conducted in the $(Ti,Nb)_2AlC$ system and the at that time newly added solid solution phase $(Ti,Hf)_2InC$ by Salama[99] et al. and Barsoum et al.[100] For instance, the formation of the Ti–Nb solid solution improved the oxidation resistance in comparison to the parent phases.[99] In the following years, the reports of new solid solution MAX phases increased significantly and the initial M-site compositions of Schuster et al.[96–98] with the addition of zirconium-based[101] phases were also applied to 312 and 413 or even higher aluminum-carbide-based systems. Interestingly, two Cr–Ti solid solution phases $(Cr_{2/3}Ti_{1/3})_3AlC_2$ (ordered phase, see Section 3.2) and $(Cr_{5/8}Ti_{3/8})_4AlC_3$ were reported,[73] even though the parent phases Cr_3AlC_2, Cr_4AlC_3, and Ti_4AlC_3, were not been predicted to be stable.[102] Recent studies on phases with three or more elements (e.g. $(Ti,Nb,Ta,V)_4AlC_3$[103]) push towards "high entropy"[104,105] MAX phases using the common transition metals of groups 4–5 leading to compounds with enhanced mechanical properties. However, "conventional" two element M-site solid solution phases still exhibit large potential as just shown with the synthesis of $(V_{1-x}Cr_x)_2GaC$,[106] a solid solution phase almost matching the Stoner criterion. In general, the synthesis and characterization of M-site solid solution phases consisting of the early transition metals that MAX phases were initially known for, have enabled tailoring specific materials properties such as oxidation resistance,[107,108] mechanical characteristics,[103,109] or thermal properties.[110] Furthermore, the research area still holds a great potential as shown in recent literature reports.[103,106] Besides, the formation of solid solution phases is not only restricted to MAX phases, they have also shown benefits for specific properties of MXenes.[111]

4.2. Later transition metals as M-elements

The property profile of solid solution MAX phases was even more broadened with the introduction of mid-transition metals, such as manganese or iron, on the M-site. In 2013, Ingason et al.[112] reported the successful incorporation of 25 at-% manganese on the M-site of Cr_2GeC thin films, resulting in the first magnetic MAX phase. Since then, and particularly after the synthesis of Mn_2GaC thin films exhibiting ferromagnetic characteristics up to $T = 230$ K in the same year,[113] many doping studies with manganese on the M-site have been conducted. As parent phases, mostly chromium-based 211 MAX phases Cr_2AC with A=Al,[114–116] Ga,[115,117,118] and Ge[115,116,119] as A-elements were studied in detail. For example, Mockute et al. synthesized $(Cr_{0.8}Mn_{0.2})_2AlC$ thin films that revealed a magnetic response significantly above room temperature.[120] This was followed by the synthesis of magnetically ordered $(Cr_{0.5}Mn_{0.5})_2GaC$ films in 2015.[121] Nonetheless, the research was not only restricted to MAX phase thin films but also bulk systems, such as conven-

tionally synthesized $(Cr_{0.94}Mn_{0.06})_2AlC$,[122] $(Cr_{0.85}Mn_{0.15})_2GaC$,[122] or $(Cr_{1-x}Mn_x)_2GeC$ $0 \leq x \leq 0.25$.[123] While the Al-based MAX phases revealed no magnetic response, the Ga-containing ones may be magnetic, whereas the Ge-based phase exhibited weak ferromagnetism with a T_C close to room temperature for a doping level of $x = 0.20$.

However, as the above cited examples have shown, the magnetic behavior of MAX phases is very complex as a consequence of their inherently nanolaminated character. Furthermore, the magnetic properties are highly dependent on the sample quality. Particularly, the latter has turned out to be very challenging due to the formation of more thermodynamically stable side phases, such as antiperovskite phases, binary phases, or other MAX phases that also influence the observed magnetic properties (comprehensively discussed by Ingason et al.).[6] In order to circumvent several disadvantages that are accompanied with conventional solid-state synthesis procedures, Hamm et al. applied microwave heating (see Section 7.1.2) to increase the doping level of manganese towards 10% and reached a doping level of 2% iron on the M-site of Cr_2AlC.[124] In 2021, Sobolev et al. were able to increase the Mn-amount even up to 16 at-% using the arc melting technique, however, the magnetic ordering is restricted to paramagnetism.[125] Other non-conventional bulk synthesis approaches were made by Siebert et al. applying a sol-gel approach to synthesize manganese-doped Cr_2GaC with a doping level up to 16%. While not in the bulk, the authors found Mn-rich areas of the MAX phase that may be magnetically ordered.[126]

Going beyond 211 systems, only the magnetically ordered 312 phase $(V,Mn)_3GaC_2$ was reported by Tao et al.,[127] whereas no examples for 413 phases can be found. This further affirms the complexity of incorporating later transition metals into the MAX phase structure. On the other hand, this also shows that this field of research is still in its infancy and provides a tremendous space for further investigation, which is also confirmed by theoretical calculations where new MAX phases containing later transition metals (e.g. Mn as a sole element) have been predicted to be stable.[128] In terms of magnetism, Tao et al.[87] synthesized chemically (see Section 3.2) and magnetically ordered rare earth-doped MAX phases that form a suitable complementation of the previously introduced late transition metal doped MAX phases.

5. Variation of A

5.1. Common A-elements

Common A-elements in MAX phases are elements from groups 13 and 14, periods 3–6, namely Al, Ga, In, Tl, Si, Ge, Sn, and Pb.[3] With regards to how often different A-elements occur in ternary MAX phases, the most common A-element is aluminum. It is found in many carbide-based MAX phases with $n = 1–3$ and the nitride MAX phases Ti_2AlN[129] and Ti_4AlN_3.[130,3] Several aluminum carbide MAX phases are easy to access by conventional solid-state reactions.[131,132] The second most common A-element

is gallium.[3,132] Most gallium-containing MAX phases are 211 phases,[3,14] except for Ti_3GaC_2, Ta_4GaC_3 and Ti_4GaC_3.[27,133] Due to its low melting point, the handling of gallium can be challenging, but transport processes are facilitated in the melt. A variety of ternary indium, tin, and germanium-containing MAX phases has been synthesized in the past.[3,131,132] There are not many silicon-based MAX phases known. Silicon forms in combination with titanium carbon-based ternary MAX phases.[131,134] Thallium and lead only form a few 211 carbides which were discovered in the 1960s.[3] i-MAX phases that were obtained experimentally are gallium or aluminum-based but indium should also be an appropriate A-element to form i-MAX phases according to predictions.[80–88,135] Previously synthesized quaternary o-MAX phases are exclusively aluminum-based compounds.[74–78] Solid solutions on the A-site have been realized in the past. Aluminum forms solid solutions with gallium in $V_2(Al,Ga)C$,[27] tin in $Zr_2(Al,Sn)C$,[136] $Ti_3(Al,Sn)C_2$,[137] and $Ta_3(Al,Sn)C_2$[138] and germanium in $Cr_2(Al,Ge)C$[139] as well as silicon in $Zr_3(Al,Si)C_2$,[140] $Cr_2(Al,Si)C$[141] and $Ti_3(Al,Si)C_2$[142] and lead in $Zr_2(Al,Pb)C$.[136] Furthermore silicon has been mixed with germanium in the quaternary compound $Ti_3(Si,Ge)C_2$.[143] Multinary MAX phases that have been prepared are $Ti_3(Al,Si,Sn)C_2$[144] and some double substitution[145–147] and higher mixed compounds[147] with mixed elements on the M- and A-sites. Mixed compositions on the A-site can also introduce more "exotic" A-elements into MAX phases, which are described in the following chapter.[3]

5.2. Exotic A-elements

Most commonly, MAX phases contain main group elements Al, Ga, and Ge as the A-element.[3,60] Less common are Si, In, Tl, Pb, and Sn[3] and the least common main group elements are P, As, S, Se, Bi and Sb.[148,149] We consider these main group elements (P, As, S, Se, Bi, Sb) including late transition metals (e.g. Cd, Zn)[150] as "exotic A-elements" and discuss them in more detail (see also Table 1). MAX phases of this type only crystallize in the 211 structures, there are no reports of respective 312 structures and beyond. Phosphorus-containing MAX phases were first synthesized in the 1960s by Boller and Nowotny (V_2PC and Nb_2PC).[149] The original synthesis description includes reacting the elemental reagents at 1000 °C but communicate no further details. An alternative approach was developed by Sinclair et al. which is based on sol-gel chemistry (see Section 7.1.1 for details).[151] Similar to the original high-temperature solid-state synthesis of V_2PC, the Nb-analog (Nb_2PC) was prepared by furnace heating at 1150 °C in inert environments.[152] Instead of phosphorous, MAX phases with As as the A-element have also been reported (V_2AsC[148] and Nb_2AsC[152]), however very little information is provided about these two phases in the original literature. For group 16 A-elements, the syntheses of Ti_2SC and Zr_2SC were achieved by melting elemental Ti/Zr, S, and C at 1600 °C, cooling to 1300 °C over the course of 3 hours and subsequent cooling to room temperature.[16] Further examples are Hf_2SC and Nb_2SC which were prepared with similar reaction conditions and maximum temperatures ranging from 1150–

Table 1. A list of MAX phases with "exotic" A-elements.

Exotic A-Site Element	MAX Phase	Reaction conditions
P	V_2PC[149,151], Nb_2PC[152]	1000–1150 °C[a]
As	V_2AsC[148], Nb_2AsC[152]	1100–1150 °C[a]
S	Ti_2SC, Zr_2SC, Hf_2SC, Nb_2SC[16,153]	1150–1600 °C[a]
Se	Zr_2SeC[153], Hf_2SeC[153], $Zr_2Se(B_{1-x}Se_x)$[62]	1500–1600 °C[a]
Sb	Ti_3SbC_2, Ti_3SbCN[32]	Sb, $CdCl_2$[c]
Sb	$Ti_3(Sb_{0.5}Sn_{0.5})CN$[32]	Sb–Sn, $CdCl_2$[c]
Sb	Nb_2SbC[32]	Sb, $CdCl_2$[c]
Bi	Nb_2Bi_2C[32]	Bi, $CuCl_2$[c]
Cd	Ti_2CdC[150]	750 °C[a]
Cd	$Ti_3Cd_2C_2$[32]	Cd, Al[c]
Zn	Ti_3ZnC_2[155]	$ZnCl_2$[b]
Zn	Ti_2ZnC[155]	$ZnCl_2$[b]
Zn	Ti_2ZnN[155]	$ZnCl_2$[b]
Zn	V_2ZnC[155]	$ZnCl_2$[b]
Zn	Nb_2ZnC[32]	Zn, $CdCl_2$[c]
Cu	$Ti_2(Al_{0.1}Cu_{0.9})N$[156]	$CuCl_2$[b]
Cu	Nb_2CuC[156]	CuI[b], Cu, $CdCl_2$[c]
Cu	$Ti_3Cu_{1-x}Al_xC2$[159]	$CuCl_2$[b]
Cu	$Ti_3Cu_{1-x}Al_xC_2$[158]	Cu[b] ball mill
Fe	Ta_2FeC[157]	$FeCl_2$[b]
Fe	Ti_2FeN[157]	$FeCl_2$[b]
Fe	Nb_2FeC[162]	$FeCl_2$[b], Fe, $CdCl_2$[c]
Fe	$Mo_2(Ga,Fe)C$[163]	Fe[b] thin film
Co	Nb_2CoC[32]	Co, $CdCl_2$[c]
Ni	Nb_2NiC[32]	Ni, $CdCl_2$[c]
Au	Nb_2AuC[32]	Au, $CdCl_2$[c]
Au	Mo_2AuC[161]	Au[b] thin film
Au	$Mo_2(Au_{1-x}Ga_x)_2C$[161]	Au[b] thin film
Au	Ti_3AuC_2[69]	Au[b] thin film
Au	$Ti_3Au_2C_2$[69]	Au[b] thin film
Au	$Nb_2(Au_{0.5}Al_{0.5})C$	Au, $CdCl_2$[c]
Ag, Sb	$Nb_2(Ag_{0.3}Sb_{0.4}Al_{0.3})C$	Ag–Sb, $CdCl_2$[c]
Ir	Ti_3IrC_2[69]	Ir[b] thin film
Rh	$Nb_2(Rh_{0.2}Sn_{0.4}Al_{0.4})C$[32]	RhSn, $CdCl_2$[c]
Pt	$Nb_2(Pt_{0.6}Al_{0.4})C$[32]	Pt_3Cd, $CdCl_2$[c]
Pt	Nb_2PtC[32]	Pt_3Cd, $CdCl_2$[c]
Pd	$Nb_2(Pd_{0.5}Sn_{0.5})C$[32]	PdSn, $CdCl_2$[c]

[a] high temperature reaction, temperature stated, [b] A-element replacement, reactant stated,[155] [c] chemical scissor, reactant stated[32]

1600 °C depending on the M-element.[16,153] Selenium-containing MAX phases have also been reported, e.g. Zr_2SeC and Hf_2SeC which were prepared at 1500 °C and 1600 °C in the case of Zr_2SeC[154] and Hf_2SeC,[16] respectively. Selenium is also an A-element in the just recently found chalcogenide-based MAX phase $Zr_2Se(B_{1-x}Se_x)$.[62] Bi and Sb (see Table 1) containing MAX

ChemPlusChem

Review
doi.org/10.1002/cplu.202300214

**Chemistry
Europe**
European Chemical
Societies Publishing

phases were synthesized just recently by using a chemical scissor-based method in which $CuCl_2$ and $CdCl_2$ were used as the chemical scissor.[32]

Another group of exotic A-elements are selected late transition metals. There are only a few reports about the synthesis by conventional high temperature solid-state methods. As an example, Jeitschko *et al.* prepared Ti_2CdC by combining elemental precursors at 750 °C for 900 h.[132] An alternative and elegant method is the replacement of a common A-element with the transition metal of a Lewis acid salt, e.g. $ZnCl_2$ and $CuCl_2$.[155,156] The initial A-element is oxidized by the salt and the reduced transition metal replaces it in the MAX phase structure. The method and reaction mechanisms are similar to the process of molten salt exfoliation by Lewis acid salts which is described in Section 7.2.2. For the replacement, smaller amounts of Lewis acid salts are used than for the exfoliation in order to avoid full removal of the A-element. Therefore, the A-element replacement can also be described as an early reaction step in the molten salt exfoliation.[155] By replacing aluminum with zinc in Ti_3AlC_2, Ti_2AlC, Ti_2AlN, and V_2AlC, the MAX phases Ti_3ZnC_2, Ti_2ZnC, Ti_2ZnN, and V_2ZnC were synthesized using $ZnCl_2$ as the Lewis acid salt.[155] Al was partially substituted by Cu in Ti_2AlN to form $Ti_2(Al_{0.1}Cu_{0.9})N$ (with $CuCl_2$) and fully substituted in Nb_2AlC to form Nb_2CuC (with CuI).[156]

In terms of functional properties, the A-element replacement method makes the synthesis of MAX phases with magnetic transition metals on the A-site possible. Relevant compounds which are magnetic are Ta_2FeC, Ti_2FeN, and Nb_2FeC. These compounds were obtained by the reaction of the respective aluminum-based precursor with $FeCl_2$. Ta_2FeC, and Nb_2FeC are ferromagnets with Curie temperatures near room temperature of 291 and 281 K, whereas Ti_2FeN has a lower Curie temperature of 208 K.[157] Another method which is besides main group elements also suitable to introduce transition metals and similar to the molten salt method is the reaction with a chemical scissor and the insertion of a new A-element by reaction with the metal. By using this method Co, Ni, Ag, Pt, Pd and Rh were introduced into MAX phases on the A-site.[32]

Higher order MAX phases with later transition metals on the A-site have also been realized. $Ti_3Cu_{1-x}Al_xC_2$ was synthesized by a partial substitution with elemental Cu[158] as well as $CuCl_2$[159] as the reactant. In this compound a partial in-plane ordering of the mixed A-elements was observed.[158,159] By reaction of a grinded mixture of Ti_3AlC_2 with elemental Cu, a MAX phase in which Cu was incorporated partially on the M- and A-site has been synthesized.[160]

For thin films, Mo_2AuC and $Mo_2(Au_{1-x}Ga_x)_2C$ have been synthesized by an A-element replacement method from thin films of Mo_2GaC and Mo_2Ga_2C. The source of the new A-element was an elemental Au layer that was applied by sputtering. For $Mo_2Au_{1.8}Ga_{0.2}C$, an in-plane ordering of gallium in the A-layers was found.[161] Ti_3SiC_2 was used as a precursor to obtain Ti_3AuC_2 as well as $Ti_3Au_2C_2$ by reaction of thin MAX phase films with thin Au films. By a further reaction of $Ti_3Au_2C_2$ with Ir films, Ti_3IrC_2 was formed.[69]

It is generally understood that exotic A-element MAX phases, namely those containing P, As, S, and Se have no reported successes of being chemically exfoliated or A-site replaced. The mechanisms/techniques that are described in Section 7.2.2 involving molten salt exfoliations are not applicable to MAX phases of this nature because most of these exfoliations involve Al. This however has the potential to change with new advancements described earlier by Huang *et al.*[32] The description of using LAMS scissors to open non-van der Waals gaps in different MAX phases and then exploit differences in redox potential between atoms is a revolutionary approach to structural editing of MAX phases.[32] This, of course, can be extended to MAX phases incorporating Si, In, Tl, Pb, and Sn. Pushing it further Huang *et al.* mention another technique that describes diffusion of atoms into interlayer atom vacancies.[32] This would be another appropriate methodology for potentially incorporating noble metals into exotic MAX phases in an elegant way.

6. Variation of X

6.1. Nitrides

When looking at the overall numbers of known MAX phases, MAX phase nitrides represent only a small part of them ($n < 15$) and are outnumbered by carbides by a factor of ten (> 150). The significant difference in these numbers can be related to challenges during the synthesis of nitrides. Besides the gaseous state under normal conditions, the nitrogen molecule exhibits partially low diffusion rates, as well as a high bonding energy that heavily inhibits direct nitridation reactions.[164] Hence, in contrary to carbides, where carbon is frequently used as an elemental precursor, binary nitride precursors are required to maintain MAX phase stoichiometry. Apart from these challenges, nitrides in general are recognized as demonstrating advantages over their carbide counterparts, such as an enhanced magnetic exchange correlation[165] or higher electronic conductivities. For instance, the latter can be observed for the Ti_2AlN phase where the nitride phase possesses this over the carbide one.[166–170] On the other hand, similar to the carbide phases, the Ti–Al system also represents the most studied system in the field of nitride MAX phases. Many synthesis protocols including property measurements have been published for the 211 system.[129,166–170] New studies also address the ability of Ti_2AlN to act as a coating material[171] or as a nanocomposite material in a MAX phase/cellulose acetate membrane.[172] Going beyond 211 phases, the Ti-based 413 phase Ti_4AlN_3 served as the precursor for the first nitride MXene in 2016,[46] which further substantiates the interest in the Ti–Al–N system. Nonetheless, the interest in nitride phases is not only restricted to the Ti-based phases. The 211 Cr_2GaN phase also represents an important nitride candidate. While most of the magnetic properties of the MAX phases arise from doping experiments (see Section 4.2), this phase exhibits, without any doping, a magnetic phase transition in form of a spin density wave (SDW) at $T_N = 170$ K.[173,174] No comparable behav-

ChemPlusChem

Review
doi.org/10.1002/cplu.202300214

Chemistry
Europe
European Chemical
Societies Publishing

ior is known for any reported carbide MAX phase. Further efforts were made to suppress the SDW state by Ge-doping experiments to induce a superconducting state in the system, however, without success.[175] Thus, Ti$_2$InN stays the only super-conducting nitride MAX phase with a transition temperature of $T_C = 7.3$ K.[176] The remaining of the reported nitride MAX phases are mostly known since the early reports on H-phases by Nowotny et al. in the 1960 s[129,132,150,177] but without any further characterization steps (Table 2). New efforts in the synthesis of nitrides were made by Kubitza et al.,[178] who have recently developed a new synthesis approach by combining the liquid ammonia method with conventional techniques to synthesize V$_2$GaN at moderate temperatures with an unusual morphology. This technique has also the potential to be applied to other nitride systems, including hitherto unknown phases, where several have already been predicted to be stable.[5] Overall, the interesting properties of already characterized MAX phase nitrides, the challenging synthesis procedures, as well as the unknown potential of hitherto unknown phase systems makes research in the field of MAX phase nitrides at least as important as work in the predominant field of MAX phase carbides.

6.2. Carbonitrides

Even more scarcely represented than nitrides are carbonitride MAX phases with less than 5 reported compounds (Table 3). However, analogous to the parent carbides and nitrides, Ti–Al-based phases are studied the most. First reports of carbonitrides reach back to the work of Pietzka et al. in the 1990s with the synthesis of Ti$_2$AlC$_{1-x}$N$_x$ ($0 \leq x \leq 1$).[179] In 2008, Scabarozi et al. synthesized the 211 and 312 phase with $x = 0.50$ and studied the thermal and electrical properties in comparison to the parent phases.[167] Here, the resistivity of the carbonitride members is significantly higher than those of the pure X-site phases due to scattering factors such as vacancies or other defects whereas the thermal conductivity is similar to the parent phases.[167],[1] On the other hand, the 211 Ti$_2$AlC$_{0.5}$N$_{0.5}$

phase exhibits enhanced mechanical properties, such as a higher hardness and stiffness than Ti$_2$AlC and Ti$_2$AlN.[169] Furthermore, it has been shown that it is possible to synthesize stable carbonitrides with at least 20 % of vacancies on the C or N site, which is not achievable for carbide phases.[180] Besides the Ti–Al-system, recent studies report the two-step synthesis of the carbonitride phase V$_2$GaC$_{1-x}$N$_x$ with $x \approx 0.5$ by combining the so-called "urea-glass route" with conventional solid-state techniques.[178] More complex carbonitrides have been synthesized by Du et al., who combined a high entropy approach on the M-site (see Section 4.1) with an X-site solid solution.[105] The carbonitride was then used as a precursor for MXenes, resulting in a product with high mechanical strains and good catalytic activities. As shown by the latter examples and the small number of reported carbonitrides, the field has immense potential to be expanded in future studies, in order to further increase the phase variety of MAX phases with the potential to obtain products possessing improved properties compared to the parent phases.

6.3. MAB phases

MAB phases are layered borides consisting of a transition metal (M), an A-group element (A), and boron (B). The difference between MAX and MAB phases is that MAB phases are borides and have different structures than MAX phases. The existence of ternary borides with the same structure as MAX phases has been predicted for Hf$_2$BiB and Hf$_2$PbB.[55] Nb$_2$SB with a MAX phase structure has been synthesized by Rackl et al.[61] A recently synthesized compound is Zr$_2$SeB, in which boron can be substituted by selenium to produce a mixed X-element compound up to 97 %.[62] Compounds with the same structure as MAX phases (P6$_3$/mmc) and boron as the X-element are classified as boride-based MAX phases instead of MAB phases.[52,61] A commonality of MAB and MAX phases is, that they have layered structures derived from 2D building blocks.[52,181] In contrast to MAX phases, the transition metals and boron building blocks do not form edge-shared octahedra. Instead, the transition metal atoms are arranged in the form of trigonal prisms which are interconnected via shared faces. Boron atoms form zigzag chains or bands of six rings. The boron-boron bonds of these formations percolate through the quadrangular faces of the transition metal prisms. Actual MAB phases have a large structural variety. Therefore, they are categorized in different classes. Most MAB phases exhibit an orthorhombic symmetry with aluminum as the A-element.[52,181] Orthorhombic MAB phases can be categorized in subgroups based on the structure models of different compounds.[52,181] The structures can be derived from binary transition metal borides. The A-atoms separate the M-B-layers in the form of single- or double-atomic sheets. Only in the MAlB (222, Cmcm)[182] structure, a double-A-element layer is present. In contrast to the double-A MAX phase (221) structure, the aluminum atoms in both sheets are shifted towards each other and they are not stacked over each other perpendicularly to the M–X-layers. The single Al-sheet structures are M$_2$AlB$_2$ (212,

Table 2. A list of reported nitride MAX phases.		
4d M-metal	Ti$_2$FeN[157]	5d M-metal
Ti$_2$AlN[129]	Ti$_2$(Al$_{0.1}$Cu$_{0.9}$)N[156]	V$_2$GaN[177]
Ti$_4$AlN$_3$[46]	Zr$_2$InN[132]	V$_2$GeN[177]
Ti$_2$GaN[132]	Zr$_2$TlN[177]	**6d M-metal**
Ti$_2$InN[132]	Hf$_2$SnN[14]	Cr$_2$GaN[150]
Ti$_2$ZnN[155]	Hf$_2$InN[177]	

Table 3. A list of reported carbonitride MAX phases.
Carbonitride phases
Ti$_2$AlC$_{1-x}$N$_x$[179]
Ti$_3$Al(C$_{1-x}$N$_x$)$_2$[167]
V$_2$GaC$_{1-x}$N$_x$[178]
(Ti$_{1/3}$V$_{1/6}$Zr$_{1/6}$Nb$_{1/6}$Ta$_{1/6}$)$_2$AlC$_{1-x}$N$_x$[105]

ChemPlusChem

Review
doi.org/10.1002/cplu.202300214

Chemistry Europe
European Chemical
Societies Publishing

$Cmmm$),[183,184] Cr_3AlB_4 (314, $Immm$),[185] M_4AB_4 (414, $Immm$),[186] and Cr_4AlB_6 (416, $Cmmm$)[187]. The Zn-A-element MAB phase Ru_2ZnB_2 also exhibits the orthorhombic structure ($I4_1/amd$).[188] Another orthorhombic MAB phase composition is 322 with the space group $Cmmm$.[189] $Fe_3Al_2B_2$ (322, $P2/m$)[190] has a monoclinic structure and is not a MAB phase.[191] The structures of orthorhombic MAB phases can be found in Figure 4. Hexagonal MAB phases are not well explored, only M_5Si_3B (M=Cr, Hf)[192] and Ti_2InB_2 (P-6 $m2$)[193] exist. But many additional hexagonal MAB phases have been predicted. Y_2SiB_8[194] is a tetragonal MAB phase. Similar to MAX phases, ordered i-MAB phases $Mo_{4/3}RE_{2/3}AlB_2$ (RE=Sc,[195] Y,[195] Ho,[196] Tb,[196] and Er[196]) (R-3 m) exist. A list of selected compounds with different symmetry that have a M_2AB_2 composition are displayed in Table 4.

Regarding magnetic properties, an advantage of MAB phases compared to MAX phases is that compounds with later transition metals are stable. Transition metals like Fe or Mn can introduce magnetic ordering. Mn_2AlB_2[200,201] ($T_N = 390$ K)[200] is antiferromagnetic, while Fe_2AlB_2[184,202,203] is ferromagnetic. Fe_2AlB_2 ($Tc = 290$ K, strong dependency on impurities)[181,203] in addition shows a strong magnetocaloric effect near room temperature.[202,204]

The so-called T_2-phases are layered borides as well and are interesting regarding magnetism.[191] In the literature they are sometimes called MAB phases[205] but mostly they are regarded as a separate class.[52,191] They crystallize in the Cr_5B_3 structure ($I4/mcm$).[206] A lot of T_2-phases like Fe_5PB_2,[207,208] Fe_5SiB_2,[207,209] Co_5PB_2,[210] Co_5SiB_2,[211] Mn_5PB_2,[210] Mn_5SiB_2[212] are ferromagnets. Shen *et al.* predicted several further layered borides which should be stable and exhibit magnetic properties. Useful for magnetocaloric cooling and sustainable energy applications are especially $Fe_3Zn_2B_2$, Fe_4AlB_4, Fe_3AlB_4, Fe_3ZnB_4, and Fe_5B_2.[191]

The layered structure of MAB phases makes them an interesting precursor for the synthesis of MBenes. Whereas the exfoliation of MAX phases into single-atomic MXenes sheets has been reported experimentally and theoretically for numerous compounds, there are only a few examples in which selective removal of the A-element from MAB phases could be confirmed. Most of the obtained substances did not form as fully exfoliated single atomic 2D-MBene sheets.[52] The only time in which the formation of fully exfoliated 2D-MBene sheets could be confirmed was for $(Mo_{2/3}Y_{1/3})_2AlB_2$.[213] Aluminum could still be selectively removed from Cr_2AlB_2,[214] MoAlB,[215,216] and Mo_2AlB_2,[217] but in these cases the product seemed to be an exfoliated bulk compound instead of a 2D-material. Cr_2AlB_2 has been etched in hydrochloric acid to obtain Cr_2B_2. The etching is confirmed by SEM images that show a morphology change from layered particles to separated sheets. A significant reduction of aluminum content below 1% is determined by EDS. For the XRD pattern, different structures of multilayer compounds with interlayered OH-groups have been calculated and compared to the XRD pattern. None of them matches completely.[214] Assignment of the reflections was more successful in a following work with lower concentrated HCl solution in which the size of the resulting sheets was determined to be below 100 nm thick.[218] Kim *et al.* and Alameda *et al.* synthesized Mo_2AlB_2 through a selective etching route from MoAlB.[215,216] Kim *et al.* removed one aluminum layer from the double layer of MoAlB directly by using an in situ-HF method (LiF/HCl).[216] Alameda *et al.* also obtained $MoAl_{1-x}B$ by removing aluminum by an NaOH etching step. The overall conversion to stoichiometrically sharp Mo_2AlB_2 was achieved by a subsequent annealing step at 1400 °C in which residual aluminum is converted to AlO_x. The product is a nano hybrid with 1–3 nm of MAB phase layers between AlO_x.[215] By using NaOH the authors also obtained Mo–Al–B-sheets with a thickness in the nanometer scale from pure MoAlB by partially etching aluminum with NaOH.[219] In another publication they observed the formation of single Mo–B-sheets after the conversion of MoAlB with different etchants which were still connected to larger intergrown Mo–Al–B particles and not fully separated. They tested the use of alkaline solution (NaOH) as well as acidic in situ-HF etching (LiF/HCl). To prevent corrosion in the Mo–B-layers, alkaline etching proved to be the most suitable method.
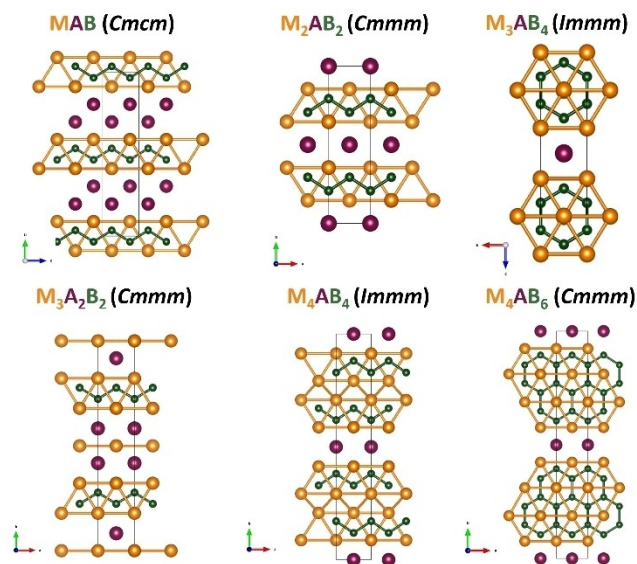
Figure 4. Structures of orthorhombic MAB phases.

Table 4. A list of experimentally available MAB Phases with a M_2AB_2 formular and their space groups.	
Compound	Space group
Fe_2AlB_2[183]	$Cmmm$
Mn_2AlB_2[185]	$Cmmm$
Cr_2AlB_2[185]	$Cmmm$
$(Fe,Mn)_2AlB_2$[197]	$Cmmm$
$(Fe,Co)_2AlB_2$[198]	$Cmmm$
$(Mn,Cr)_2AlB_2$[199]	$Cmmm$
Ti_2InB_2[193]	P-6 $m2$
$Mo_{4/3}Sc_{2/3}AlB_2$[195]	R-3 m
$Mo_{4/3}Y_{2/3}AlB_2$[195]	R-3 m
$Mo_{4/3}Ho_{2/3}AlB_2$[196]	R-3 m
$Mo_{4/3}Tb_{2/3}AlB_2$[196]	R-3 m
$Mo_{4/3}Er_{2/3}AlB_2$[196]	R-3 m

ChemPlusChem

Review
doi.org/10.1002/cplu.202300214

**Chemistry
Europe**
European Chemical
Societies Publishing

Generally, this result demonstrated that the formation of fully separated single Mo–B sheets should indeed be possible.[217] The synthesis of $Mo_{4/3}B_2$ was achieved by treatment of the *i*-MAB compound $(Mo_{2/3}Y_{1/3})_2AlB_2$ with concentrated hydrofluoric acid. Besides the *A*-element, yttrium was removed from the structure. Thereby ordered vacancies formed within the metal-boron planes, similar to the etching of rare earth containing MAX phases. In this work delamination was conducted to produce pure single sheet MBene samples.[213] For the hexagonal MAB phase Ti_2InB_2, the removal of indium by thermal treatment in vacuum was reported. In addition to the indium release, a change in the structure of the Ti–B lattice was observed as well. The product was a layered orthorhombic (*Cmcm*) boride with the sum formula TiB.[193] Besides aluminum, the removal of molybdenum, silicon, and boron from Ti_4MoSiB_2 resulted in the formation of TiO_xCl_y single sheets.[205]

The fact that the synthesis of completely phase-pure exfoliated samples has not been achieved often in the past makes the experimental determination of magnetic properties difficult. Magnetic properties for Cr_2B_2,[220–222] Mn_2B_2[221,223] and Fe_2B_2[50,220,224] have been predicted, but for Fe_2B_2[50,220,224] and Cr_2B_2[220–222] the literature does not show consistent predicted properties.[52] This result is due to different methods and different assumptions in the calculations.[52] Cr_2B_2 and Fe_2B_2 could both be ferromagnetic or antiferromagnetic.[50,220–222,224] Ferromagnetic properties have been predicted for Mn_2B_2[221,223] which would signify that removal of the *A*-element would change the magnetic properties from antiferromagnetic for Mn_2AlB_2[200,201] to ferromagnetic for Mn_2B_2.[221,223]

A future challenge in the field of MAB phases in general is the extension of the family towards new structures especially with regard to non-orthorhombic structures such as hexagonal structures for instance. Regarding the MBene synthesis, there are a lot of challenges that have to be tackled because most MAB phases could not be converted to single 2D-MBene sheets yet. The testing of new exfoliation methods could be a crucial step into this direction.

7. Synthesis strategies

7.1. MAX phases

Synthesis strategies for the preparation of MAX phases are almost as vast and diverse as the compounds themselves. Two larger categories one may define are the synthesis of bulk vs. thin film MAX phases. The respective methods differ significantly and need to be discussed separately. Here, we will focus almost exclusively on the preparation techniques of bulk MAX phases and will only briefly summarize thin film techniques. The reader is referred to a comprehensive review article that discusses thin film syntheses in detail.[60]

Synthesis methods for thin film vs. conventional bulk MAX phases are fundamentally different, in that the latter generally operates close to thermodynamic equilibrium while the former proceeds far from thermodynamic equilibrium. Please note that there are exceptions for both cases (see discussions in

Section 7.1.2.). Consequences for the different synthesis principles are that thin film MAX phases can be produced at much lower temperatures than are required for bulk MAX phase formation. For example, 211 MAX phases can be sputter-deposited at temperatures between 450 °C and 700 °C, while higher order MAX phases require temperatures up to 800–1000 °C (that are still lower than what is needed in the bulk). A similar finding applies to the synthesis of bulk phases where 312 and 413 MAX phases, e.g., Ti_3AlC_2[225] and Ta_4AlC_3,[226] form by annealing their respective 211 phases. Also, metastable phases can be accessible as thin films.

Physical Vapor Deposition (PVD) is commonly used to access MAX phase thin films. The typical protocol is based on sputtering from elemental targets for *M* and *A* and graphite, and a large number and variety of MAX phases were prepared that way, e.g., Ti_2AlC, Ti_3AlC_2,[227,228] Ti_2SnC, Ti_3SnC_2, Ti_2GeC, Ti_3GeC_2, Ti_4GeC_3,[227] Ti_4SiC_3,[134,229,230] and many more. Thin film growth by PVD has led to the discovery of the first magnetic MAX phase, Mn_2GaC,[113] that, as of now, is only accessible in the form of thin films. Additional MAX phase thin films with magnetic order have also been synthesized by these techniques opening an exciting new field/family of magnetic MAX phases.[6]

7.1.1. Conventional heating

Carbide and (carbo)nitride synthesis requires inert conditions (oxygen and moisture-free) to prevent the formation of competing oxide phases. This is routinely done in solid-state syntheses. In the original work on the so-called "H-phases", Jeitschko *et al.* synthesized many alloys by annealing mixtures of the elements in evacuated quartz ampoules at 1000 °C for up to 12 days.[231] Around 30 years later, Barsoum and El-Raghy prepared MAX phase Ti_3SiC_2 by cold pressing Ti, C, and SiC (180 MPa) and subsequent hot pressing at 1600 °C for 4 h (40 MPa).[22] Reactive hot pressing was also used for the 413 nitride phase Ti_4AlN_3 whereas TiH_2, TiN and AlN acted as starting materials.[130] This technique is still used for MAX phase synthesis leading to hitherto unknown family members[232–234] including a recently discovered ordered *i*-MAX phase.[86] Another widely used technique is self-propagating high-temperature synthesis (SHS). A part of a mixture of solid (elemental) starting materials is ignited which is followed by a cascade of exothermic reactions that provide the necessary energy for the reaction to occur. The precursors can further be activated by ball-milling (mechanically activated SHS) prior to heating. Examples of MAX phases that have been prepared by these methods are Ti_2SnC,[235] Ti_3SiC_2,[236–238] and Ti_2AlC/Ti_3AlC_2.[239–241] Very high temperatures can also be reached by arc melting where an electric arc is generated that can manually be moved across precursors that will melt together. Typically, multiple melting steps are conducted and the homogeneity of the product can be an issue, hence often an additional annealing step is added, e.g. in the case of Ti_3SiC_2.[242] More recently, the molten salt shielded synthesis/sintering (MS3) process has been developed[243] where potassium bromide (KBr) is used as a reaction medium that gas-tightly encapsulates the precursor

ChemPlusChem

Review
doi.org/10.1002/cplu.202300214

Chemistry
Europe
European Chemical
Societies Publishing

mixture protecting it from oxidation. This setup allows for reaction temperatures well above 1000 °C, that are necessary for the formation of most ceramic compounds making MAX phases accessible, e.g., Ti₂AlN and V₂AlC.[244] After the synthesis, the sample is washed with water and filtered to remove the salt.

All of the above discussed methods qualify as (high temperature) solid-state methods utilizing solid precursors (elemental or binary). The reaction temperatures are provided through conventional radiant heating in furnaces. Different heating transfer mechanisms are also possible and discussed in Section 7.1.2 as non-conventional heating techniques. Prior to that, another alternative and newly developed approach will be discussed which involves wet chemical processing. In contrast to solid-solid reactions, syntheses in liquid phase benefit from the intimate mixing of the precursors which enhances diffusion tremendously and oftentimes lowers reaction temperatures. Sol-gel chemistry is well known for the synthesis of oxides. However, it had not been used excessively for the synthesis of non-oxides. Inspired by Giordano *et al.*,[245] Siebert and Birkel developed a sol gel-based approach starting with water-soluble metal precursors and varying gel-building agents as the carbon and/or nitrogen source. They successfully prepared MAX phases Cr_2GaC,[246] Cr_2GeC, V_2GeC[247] and V_2PC[151] as well as hitherto unknown carbonitride phases, e.g., $V_2GaC_{1-x}N_x$[178] and $Cr_2GaC_{1-x}N_x$. Despite the perfectly mixed reactants, quite high reaction temperatures (around 1000 °C) are still necessary for the MAX phases to form. In a detailed analysis, the reaction mechanism was unraveled, which involves the carbothermal reduction of amorphous oxide species followed by subsequent reaction with graphitic carbon to form the carbide and carbonitride product.[248] Besides, gel-builders can be used, as shown for the synthesis of V_2PC (Figure 5).[151] One of the perks of starting with a gel is that it can be processed into different morphologies and shapes, which is not easily possible when working with solids/powders. This was demonstrated by the synthesis of amorphous hollow carbon microspheres that are decorated with Cr_2GaC particles[246] as well as the synthesis of Cr_2GaC (hollow) microspheres, thick films[249] and carbonaceous microwires.[250]
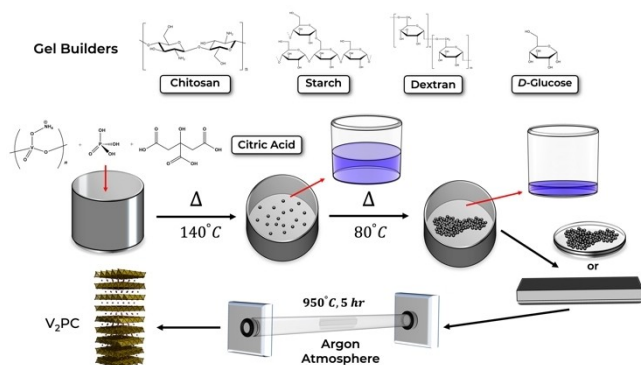
This shows that the sol-gel-based approach is largely applicable to a variety of MAX phases and unlocks unique morphologies that can be tailored for specific purposes/applications.
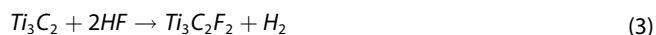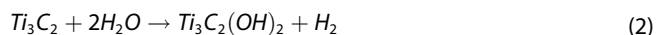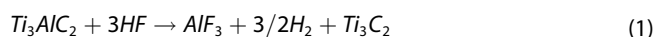
7.1.2. Non-Conventional heating

While conventional furnace heating relies on radiant heating by heating the samples "from the outside in" placing them into a heated space, inverse heating profiles ("from the inside out") or combinations of both are accessible by non-conventional heating techniques. Two examples are (solid-state) microwave heating and spark plasma sintering.[251] Microwave chemistry is well established and understood for liquid phase reactions which will not be discussed further. However, some solids also couple strongly with microwave radiation heating up rapidly and creating very high reaction temperatures.[252–254] In these cases, the reactants are heated intrinsically and, when combined with a susceptor material that surrounds the reaction mixture and couples with microwave radiation very efficiently. Temperatures easily exceeding 1000 °C are reached within 1–2 minutes. Graphite couples particularly well with microwave radiation making carbides ideal target compounds to be synthesized with microwave heating. MAX phase examples include V_4AlC_3,[255] Cr_2AlC,[124] and V_2AlC.[256]

Spark Plasma Sintering (SPS) is a valuable alternative to (reactive) hot pressing which has been used successfully for MAX phase densification and syntheses.[257] Hot pressing relies on radiative heating, typically making it a relatively slow process. During spark plasma sintering, an electric current is driven through the die, and the sample if it is conductive, leading to local Joule heating effects.[258] Like microwave heating, the reactants are heated intrinsically and extrinsically at the same time leading to fast and efficient heating profiles. Examples of MAX phase synthesis by SPS include Ti_3SiC_2,[259] Cr_2AlC,[260] Ti_3AlC_2 and Zr_3AlC_2.[261] The latter are fabricated starting from transition metal hydrides, which have the advantage of releasing hydrogen gas during the synthesis providing a reductive atmosphere and protecting the transition metals from oxidation.

7.2. MXenes

7.2.1. Acid Etching

MXene exfoliation though acid etching is separated into two steps, etching and delamination. The etching step removes the *A*-element between the lamellae, usually employing hydrofluoric acid (HF). HF is the most prevalent etchant, as it is selective for the most common *A*-elements, such as Al and Si. The etching of Ga is discussed later in this chapter. For the synthesis of Ti_3AlC_2, the process has been simplified to these steps:

Figure 5. A schematic of the sol-gel process using alternative carbon sources. Reprinted (adapted) with permission from {Inorg. Chem. 2022, 61, 43, 16976–16980}. Copyright {2022} American Chemical Society.

$$Ti_3AlC_2 + 3HF \rightarrow AlF_3 + 3/2H_2 + Ti_3C_2 \tag{1}$$

$$Ti_3C_2 + 2H_2O \rightarrow Ti_3C_2(OH)_2 + H_2 \tag{2}$$

$$Ti_3C_2 + 2HF \rightarrow Ti_3C_2F_2 + H_2 \tag{3}$$

This leaves the MXene sheets which are bound by van der Waals forces. In order to delaminate the lamellae to create single and few-layer MXene sheets, an intercalant is used to fill and expand the space between the lamellae in order to weaken the van der Waals forces. With mechanical agitation from stirring or sonication, the sheets separate and are suspended in a colloidal solution. Because this approach is relatively simple, large-scale synthesis is achievable for MXenes produced through exfoliation. However, there is little consistency with acid-based wet etching, as HF does remove some *M*-elements as well. This can leave defects along the MXene surface, affecting the functionality and stability of the final product. The process is schematically illustrated in Figure 6.

Like concentrated HF, the addition of HCl to create a dilute HF mixture has become a popular technique as it combines the etching power of fluoride ions, but reduces the harshness of the treatment, usually leading to more-intact products.[262] The surface chemistry also changes as new etchants are used, meaning that along with the usual −F, −O, and −OH functional groups, −Cl is also present. Reducing the concentration of HF does not affect its ability to remove the *A*-layer if the etching time is adjusted accordingly.[263,264]

The use of *in-situ* HF etchants, made with fluoride salts and HCl, mitigates the handling of toxic HF. Possible fluoride salts for this technique can range from alkali metal salts (LiF, NaF, KF)[265,266] to ammonia fluorides (NH$_4$F, NH$_4$HF$_2$).[265,267]

In the case of Ti$_3$AlC$_2$ exfoliation, the *in-situ* HF method introduces alkali metal ions into the etching solution, which can act as an intercalant for the resultant multilayered Ti$_2$C$_2$T$_x$ layers. This means that for this specific MAX phase, the etching and delamination process occurs simultaneously and thus the MXene can be collected as single- and few-layer- products after a single treatment. All that is needed to delaminate the sample is simply shaking the product after processing instead of using harsh agitation or sonication; a technique referred to as minimally intensive layer delamination (MILD).[263,264] *In-situ* HF etching and MILD for the combined etching and delamination only works for Ti$_3$AlC$_2$ and has not been successful in other species, though *in-situ* HF can still be used for standalone etching.[263]

Additionally, due to the high toxicity of hydrofluoric acid, it is crucial to find other appropriate etchants. Wang *et al.* showed that pure concentrated hydrochloric acid without fluoride salts can serve as an etchant for MAX phases.[93] They demonstrated this experimentally by removing gallium from Mo$_2$Ga$_2$C to obtain the MXene Mo$_2$CT$_x$. A further experiment was conducted with Cr$_2$AlC as the MAX phase precursor. The reactions were carried out at 140 °C and 150 °C in a Teflon autoclave. They predicted that several further Al- and Ga-based MAX phases are exfoliable by pure hydrochloric acid. First-principal calculations were based on the comparison of the chemical potential of the *A*-element in the MAX phase and the respective forming *A*-element-chloride species. Promising aluminum-based precursors for HCl etching are TiVAlC, Nb$_2$AlC, Ta$_2$AlC and V$_2$AlC. The calculations showed that Cr$_2$AlC is the most suitable aluminum containing precursor for MXene synthesis. The Ga-based MAX phases which are predicted to be etchable by pure hydrochloric acid are Cr$_2$GaC, Mo$_2$GaC, Mo$_2$Ga$_2$C, and Mn$_2$GaC. Therefore, this new method cannot be applied to the Al-*A*-element MAX phases V$_4$AlC$_3$, Nb$_4$AlC$_3$, Ta$_4$AlC$_3$, Ti$_2$AlN, Ti$_4$AlN$_3$, Ti$_3$AlC$_2$, Nb$_3$AlC$_2$, and Ti$_5$Al$_2$C$_3$ as well as to the Ga-based MAX phases Nb$_2$GaC, Ta$_2$GaC, Ti$_2$GaC, Ti$_2$GaN, Ti$_3$GaC$_2$, Ti$_4$GaC$_3$, V$_2$GaC, V$_2$Ga$_2$C.[93]

Not trivial to understand is why Mo$_2$Ga$_2$C can be exfoliated relatively easily in hydrofluoric acid within several days,[268,269] whereas Mo$_2$GaC seams unaffected by the treatment under the same harsh conditions.[68] The structure of Mo$_2$Ga$_2$C is similar to Mo$_2$GaC. The Mo−C-layers are the same but instead of one, Mo$_2$Ga$_2$C has two Ga-layers.[66] Mo$_2$GaC is also unique because it does not react when submerged in HF. Other not-exfoliable MAX phases instead dissolve completely when submerged into HF.[68] Björk *et al.* explained this behavior by the reaction mechanism. In Mo$_2$Ga$_2$C, a cyclic four-step mechanism takes place in which the removement of the first Ga-atom from one layer is in fact endergonic but removement of the second neighboring atom from the other layer is exergonic and in combination with the exergonic bonding of Mo to surface terminating oxygen atoms the driving force for the reaction. In Mo$_2$GaC only the endergonic removement of the first Ga-atom from one layer could take place which predominates the exergonic termination of the surface.[68] Hu *et al.* explained the exfoliability of Mo$_2$Ga$_2$C with a negative reaction energy for the
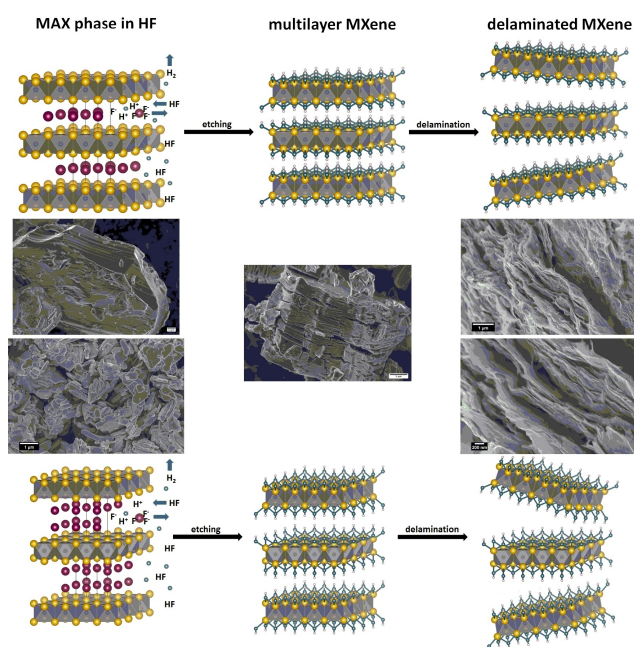
Figure 6. Schematic of the exfoliation process of a 211 (top) and 221 (bottom) MAX (−like) phase in hydrofluoric acid with SEM pictures of the respective MAX phase, multilayer MXene and exfoliated sheets next to the schematic figures. Orange: *M*-atoms, black: *X*-atoms, purple: *A*-atoms, turquoise: terminating atoms, white: H-atoms (presence depends on terminating atom which is bound to *M*).

ChemPlusChem

Review
doi.org/10.1002/cplu.202300214

**Chemistry
Europe**
European Chemical
Societies Publishing

process in contradiction to a positive reaction energy of Mo_2GaC and hydrofluoric acid.[270]

Regarding magnetic properties, the exfoliation of later transition metal MAX phases is interesting but often challenging. Khazaei et al. found by calculations that the MXenes Cr_2C and Cr_2N should be ferromagnetic, but functionalization can change the magnetic properties. Ferromagnetism should remain in the surface terminated MXenes Cr_2CF_2, $Cr_2C(OH)_2$, Cr_2NF_2, $Cr_2N(OH)_2$, and Cr_2NO_2.[271] The fact that the formation of Cr_2CT_x by removement of gallium from Cr_2GaC is not possible could be explained by the work of Tran et al. DFT calculations showed that the formation of Cr and Cr_3C_2 has a lower reaction energy than the MXene formation and therefore these products form instead of an MXene. This was found in accordance with experimental results.[272] Experimentally, Cr_2AlC on its own has been exfoliated to an MXene by fluoride free methods in the past. These methods were electrochemical exfoliation[273] as well as the exfoliation by a mixture of $FeCl_3$ and tartaric acid.[274] Experimental evidence that aluminum could be removed from Cr_2AlC by the treatment with pure hydrochloric acid under hydrothermal conditions has been provided in the work of Wang et al. by a significant decrease of the Al-amount in EDS spectra and a layered structure on SEM pictures.[93] The literature is not clear about the possible Al-etching by HF from Cr_2AlC. A very recent work describes the exfoliation of Cr_2AlC by in-situ-HF (NaF/HCl) at 9 °C.[275] SEM images show separated layers and EDS as well as XPS data show a significant reduction in Al-peak intensities after the treatment. The powder diffraction pattern on the other hand shows mainly the formation of CrC. The (002) reflection has no increased intensities and is shifted to higher instead of lower 2θ angles. A shift to lower angles would be expected for MXene formation. Tran et al. in contrast obtained a different result for their exfoliation experiments. They observed a decrease of MAX phase reflection intensities without an increase of 00 l-reflection intensities or a shift in the XRD pattern and the particles in the SEM images looked slightly dissolved rather than exfoliated.[276] Their experimental results are in good alignment with theoretical findings that were provided by Khaledialedusti et al. who calculated the exfoliation energies from the total energies of the MAX phases, MXenes and the A-elements. They found Cr_2AlC to be inexfoliable.[277] Also the calculations of Björk et al. led to the conclusion that Cr_2AlC is not exfoliable by HF.[68] In their calculations they tried to include a row of factors which can determine the success or failure of HF exfoliation. They found the free energy of exfoliation to be a good prerequisite to predict if exfoliation is possible or not. Regardless if termination groups are included in the calculation or not, the calculated free energies determine Cr_2AlC to be not exfoliable. Björk et al. also took the energies for dissolved species into account for an additional more accurate calculation. They compared how likely the solvation of M- or A-atoms in a first initial exfoliation-step is in which a vacancy is formed in the MAX phase. For Cr_2AlC they found that Cr as well as Al dissolve in HF which results in complete destruction of the MAX phase instead of the desired exfoliation.[68] Interestingly, the synthesis of MAX phases with two M-elements in which chromium is the major M-element has

been achieved fully for Cr_2TiAlC_2.[74,278] Antiferromagnetism has been predicted prior to experimental investigation for $Cr_2TiC_2T_x$ with $-F$ or $-OH$-termination groups.[279] The resulting synthesized MXene shows a magnetic transition at 30 K which is not observable in the respective MAX phase.[74] $Cr_2VC_2T_x$ with $-F$, $-OH$ or $-O$ as termination groups has been predicted to be ferromagnetic.[279] Naguib et al. could provide evidence that $(V_{0.5}Cr_{0.5})_3AlC_2$ can be exfoliated by HF but they could not produce a purified MXene sample.[34] No magnetic properties have been determined experimentally on Cr–V–C–MXenes due to the lack of experimental accessibility. Thus, $Cr_2TiC_2T_x$ is the only MXene known to date in which magnetic interaction has been measured.[74]

7.2.2. Lewis acid-based molten salt exfoliation

Besides HF-involving etching methods, there is a need for additional etchants. One reason is the toxicity of HF. Another crucial factor is that some MAX phases can not be etched by HF.[276,277] Recently, apart from fluoride-based molten salt etching, fluoride-free transition metal salts which are Lewis acids have been found to be good etchants for a row of different mainly carbide-based MAX phases including different A- and M-elements and some nitride-based phases.[155,280,281] The possibility to etch a larger variety of A-elements makes this new underexplored etching method very attractive. Molten salt etching is based on a redox reaction between the A-element and a transition metal salt. The noble transition metal etchant cation gets reduced to the metallic state. The A-element is therefore oxidized and dissolved in the molten salt mixture, thereby removed from the MAX phase.[280,282] Besides the transition metal salts, alkaline metal salts which do not participate in the reaction form eutectic mixtures that function as a flux.[280,281]

The possibility of successful MXene formation by oxidation of the A-element through specific transition metal salts can be determined by calculating Gibbs free energies from the redox potentials. This calculation has been conducted for a temperature of 700 °C. The redox potentials of the considered metal salts decrease in the order: Cu^{2+}/Cu, Ni^{2+}/Ni, Ag^+/Ag, Co^{2+}/Co, Fe^{2+}/Fe, Cd^{2+}/Cd, Mn^{2+}/Mn.[280,282] For the A-element aluminum, all selected Lewis acids are suitable etchants which has been proven experimentally[155,280,281] except for the case of the manganese salt. Li et al. etched titanium aluminum carbides by the chloride salts of Cd(II), Cu(II), Co(II), Fe(II) and Ni(II) as well as salts of other halides, namely $CuBr_2$ and CuI. Furthermore, they reported about the etching of the carbonitride Ti_3AlCN by $CuCl_2$. For Nb_2AlC, Li et al. used AgCl as an etchant.[280] Dong et al. synthesized Nb_2CT_x by the exfoliation of Nb_2AlC by $CuCl_2$ in a mixture of NaCl and KCl at temperatures between 650 °C and 800 °C.[281] For Zn as the A-element, only Mn salt is not suitable. All of the other salts are suitable redox reaction partners with regard to the calculations and experiments.[280] For the removal of Zn from Ti_3ZnC_2, Li et al. showed that Cd(II), Fe(II), Cu(II), Co(II), Ni(II) and Ag(I) chloride salts are appropriate etchants.[280] $ZnCl_2$ has proven to be a suitable salt for exfoliation of Ti_3AlC_2,

Ti_2AlC, Ti_2AlN, and V_2AlC. The mechanism to attain the MXene is an *A*-element replacement of Al by Zn in the first step which produces the respective MAX phase with Zn on the *A*-site. This step is followed by the actual etching of the obtained Zn-MAX phase. To achieve the etching reaction after the *A*-element replacement, a higher reaction time at 550 °C in 6 eq. of $ZnCl_2$ is required.[155] For the *A*-elements Si and Ga, all Lewis acids except for manganese salt have the necessary redox potential to oxidize them, but only Cu^{2+}/Cu has experimentally[280] been investigated as an etchant. The etching of gallium by the molten salt route is described but not much experimental evidence is provided. For the *A*-element Si this has been proven by the exfoliation of Ti_3SiC_2 by $CuCl_2$.[280] For In and Ge as *A*-elements, all considered Lewis acids with the redox potential of Co^{2+}/Co and higher can be used as oxidants for the MXene synthesis. Even though, no reports about experiments for the etching of In- and Ge-containing MAX phases by fluoride free molten salt routes can be found in literature. For the oxidation of Sn, the redox potential must be at least as high as the redox potential of Ag^+/Ag, but no reports about experimental realizations are available.[280,282]

In 2023, Ding *et. al.* furthered the exploration of Lewis acidic molten etching that allowed selectivity in surface terminating groups and structural editing and reconstruction of the MAX phase.[32] They deem the elemental and cationic molten salt elements to be "scissors," capable of selectively removing A-elements. This leaves behind MXene sheets which can then be terminated with a chosen anion (−S, −Se, −Te, −P, −Sb, −Cl, −Br, −I) or reconstructed into a MAX phase with a new A-element (Sb, Au, Pt, Pd, Rh, Ag, V, Bi, Ga).[32] Using this method, they were able to etch a MAX phase from Ti_3AlC_2 to $Ti_3C_2Cl_2$ and then reconstruct a variant MAX phase from $Ti_3C_2Cl_2$ to either Ti_3GaC_2, Ti_3AlC_2, Ti_3SnC_2, or $Ti_3Cd_2C_2$. Additionally, they could use this method to etch Ti_3AlC_2 from $Ti_3C_2T_x$ and then recover the original MAX phase after three cycles.[32]

A disadvantage of the molten salt method is the formation of metal side phases from the former transition metal salt. Depending on the selected element, etching without destruction of the MXene is difficult, especially for noble metals (no tendency to oxidize). It has been reported that aqueous ammonium persulfate (APS)[280,281] can be used to oxidize and dissolve copper and aqueous $FeCl_3$[280] solutions. Zinc can be dissolved by diluted HCl.[155] After removing the metal side phase, the multilayer MXenes can be delaminated by treatment with tetrabutylammonium hydroxide (TBAOH) to obtain a colloidal MXene-solution, which has been shown for the delamination of $Ti_3C_2T_x$ by $CuCl_2$ etching.[283]

7.2.3. Alternative Exfoliation Techniques

Besides the wet acid and molten salt methods, there are a lot of alternative etching methods that have been successfully used. Fluoride-free synthesis techniques are more attractive options for scaling up MXene synthesis, as these avoid exposure to HF and other fluoride-based compounds. In 2017, the electrochemical etching of Ti_2AlC in an HCl aqueous solution produced

Ti_2CT_x with no fluoride terminations and larger surface area.[284] Later, Ti_3AlC_2 was etched electrochemically in a mixture of NH_4Cl and TMAOH, which formed neutral NH_4OH and NH_4^+ cations that interleaved the $Ti_3C_2T_x$ layers so single- and double-layer sheets could be collected after brief sonication.[285] This technique is applicable to other MAX phase exfoliations, including Cr_2AlC and V_2AlC, when thermally assisted.[273]

Exfoliation in alkali media is also possible. In one study, researchers used a hydrothermal process where Ti_3AlC_2 is treated with NaOH. The hydroxide groups react with aluminum to form dissolvable $Al(OH)_4^-$, which can be easily washed away, leaving behind multilayered $Ti_3C_2T_x$, with Na^+ ions spacing apart the MXene layers in the final product.[286] When intercalated with DMSO, few-layer MXenes can be collected.

Halogen and interhalogen etching is another route that allows selective removal of aluminum.[287] Bromide and iodide ions readily form $AlBr_3$ and AlI_3, respectively and do not react with the *M*-element, which is ideal for exfoliation. These byproducts are washed away in either non-polar solvents (in the case of $AlBr_3$), tetrabutylammonium salts, or acetonitrile (in the case of AlI_3), leaving behind MXenes with surface termination corresponding to the halides of choice along with the usual −O and −OH terminations.[288]

Since 2020, there have been new and creative approaches to MAX phase exfoliation that have broadened the available options for fluoride-free synthesis. The exfoliation of Mo_2Ga_2C can be conducted by UV radiation in phosphoric acid due to its UV-responsive properties.[289] Reduction of sulfur as the *A*-element was achieved by use of a hydrogen/argon mixture under thermal treatment.[290] The exfoliation of aluminum-containing MAX phases is also possible by using an acoustic excitation[291] or algae extraction.[292]

The successful application of alternative etching methods shows that there is still a lot of room to explore the exfoliation of MAX phases and a great chance to exfoliate MAX phases that could not be converted to MXenes yet. The new and more exotic etching methods should be further investigated and be applied to a larger variety of *A*-elements. Nevertheless, the search for new methods should continue.

8. Summary and Outlook

MAX phases and MXenes pose exciting playgrounds and challenges for different scientific disciplines ranging from synthetic chemists to theoreticians, materials scientists, physicists, and engineers. Both classes are particularly fascinating due to their broad property profile. While MAX phases possess the ability to combine metallic and ceramic characteristics within one substance class, their exfoliation into MXenes enables the preparation of 2D materials with exceptional electronic properties. A long list of ternary MAX phases has been synthesized in the form of bulk compounds and thin films. A variety of synthesis techniques are applicable. For bulk phases, high temperatures are typically required for MAX phase formation to occur, and it is a major challenge to fully avoid the existence of binary side phases in the products. While it is

tempting to mainly focus on the functional properties of both materials classes, there are many fundamental issues that still need to be tackled. MAX phases are highly variable in terms of their chemical composition, many additional members have been theoretically predicted and there is no shortage of potential new solid solutions (quaternary or even quintenary compounds). Particularly, (carbo)nitride MAX phases are highly understudied. Experimentally, the discovery of new MAX phases is mostly limited by the time required to run high-temperature solid-state reactions. Here, microwave heating can be a valuable time-saving alternative to conventional furnace reactions. For carbide and carbonitride phases, graphite is a suitable precursor which couples efficiently with the microwave radiation providing internal heating within the reaction mixture. Care has to be taken in regard to reducing the amount of side phases and the identification of small amounts of side phases if they can't be suppressed completely. *M*-site solid solutions of MAX phases are not rare, particularly in the field of magnetic MAX phases. Going forward, *A*-site solid solutions should also be tackled as they promise further tuneable properties. For all solid solution MAX phases, especially for carbonitrides, multiple characterization techniques need to be combined to confirm successful formation of compounds with mixed metal and/or carbon/nitrogen occupancies. Most MAX phase reports focus on 211 phases and variations thereof. Higher order MAX phases, i.e., 413 or even 514 phases, are less common and less explored. Identification based on X-ray powder diffraction is often challenging due to the existence of multiple overlapping peaks. Based on very preliminary insights into one of the few 514 MAX phases, we should expect deviations from the $P6_3/mmc$ crystal structure, which is interesting for crystallographers and solid-state chemists.

The 2D siblings of MAX phases, MXenes, are responsible for the renewed attention that has been paid to MAX phases in the last decade. MAX phases are a path to access MXenes, and as their precursors they dictate the chemical composition of the exfoliated/delaminated structures. Therefore, many more members of the MXene family are expected to be synthesized, especially moving beyond Ti-based phases and carbides. One of the big challenges is the exfoliation of non-Al containing MAX phases; although there are few examples of the chemical exfoliation of MAX phases with *A*-elements other than aluminum, extending the possibilities further will be advantageous for producing new (versions of) MXenes. To take full advantage of the breadth of MAX phases that can potentially be converted into new MXenes, additional efforts should be directed towards chemical etching of MAX phases with *A*-elements that have not been etched today. It has to be noted though, that different etchants will further increase the complexity of the exfoliated compounds because they can affect other MXene characteristics, such as the surface groups/chemistry, flake size, defects, etc. Therefore, one of the biggest challenges in MXene research is not only the synthesis of new members of the family, but also to develop a fundamental understanding of the connection between synthesis/exfoliation parameters of MXene characteristics and functional properties.

Conflict of Interests

The authors declare no conflict of interest.

Data Availability Statement

Data sharing is not applicable to this article as no new data were created or analyzed in this study.

[1] M. W. Barsoum, *MAX Phases: Properties of Machinable Ternary Carbides and Nitrides* John Wiley & Sons, Ltd, **2013**.
[2] B. Anasori, Y. Gogotsi, *2D Metal Carbides and Nitrides (MXenes)*, Springer, Berlin, **2019**.
[3] M. Sokol, V. Natu, S. Kota, M. W. Barsoum, *Trends Chem.* **2019**, *1*, 210–223.
[4] M. Bugnet, M. Jaouen, V. Mauchamp, T. Cabioc'h, G. Hug, *Phys. Rev. B* **2014**, *90*, 195116.
[5] D. Ohmer, G. Qiang, I. Opahle, H. K. Singh, H. Zhang, *Phys. Rev. Mater.* **2019**, *3*, 53803.
[6] A. S. Ingason, M. Dahlqvist, J. Rosén, *J. Phys. Condens. Matter* **2016**, *28*, 433003.
[7] A. VahidMohammadi, J. Rosen, Y. Gogotsi, *Science* **2021**, *372*, 6547.
[8] A. Sohan, P. Banoth, M. Aleksandrova, A. Nirmala Grace, P. Kollu, *Int. J. Energy Res.* **2021**, *45*, 19746–19771.
[9] M. Hu, H. Zhang, T. Hu, B. Fan, X. Wang, Z. Li, *Chem. Soc. Rev.* **2020**, *49*, 6666–6693.
[10] Y. Gogotsi, B. Anasori, *ACS Nano* **2019**, *13*, 8491–8494.
[11] Per.O. Å. Persson, J. Rosen, *Curr. Opin. Solid State Mater. Sci.* **2019**, *23*, 100774.
[12] M. Alhabeb, K. Maleski, B. Anasori, P. Lelyukh, L. Clark, S. Sin, Y. Gogotsi, *Chem. Mater.* **2017**, *29*, 7633–7644.
[13] C. Lamiel, I. Hussain, J. H. Warner, K. Zhang, *Mater. Today* **2023**.
[14] M. W. Barsoum, *Prog. Solid State Chem.* **2000**, *28*, 201–281.
[15] C. M. Hamm, C. S. Birkel, in *Comprehensive Inorganic Chemistry III*, Elsevier, **2023**, 278–289.
[16] H. Kudielka, H. Rohde, *Z. Kristallogr.* **1960**, *114*, 447–456.
[17] V. H. Nowotny, *Prog. Solid State Chem.* **1971**, *5*, 27–70.
[18] W. Jeitschko, H. Nowotny, *Monatsh. Chem.* **1967**, *98*, 329–337.
[19] H. Wolfsgruber, H. Nowotny, F. Benesovsky, *Monatsh. Chem.* **1967**, *98*, 2403–2405.
[20] H. Nowotny, S. Windisch, *Annu. Rev. Mater. Sci.* **1973**, *3*, 171–194.
[21] J. J. Nickl, K. K. Schweitzer, P. Luxenberg, *J. Less-Common Met.* **1972**, *26*, 335–353.
[22] M. W. Barsoum, T. El-Raghy, *J. Am. Ceram. Soc.* **1996**, *79*, 1953–1956.
[23] M. W. Barsoum, D. Brodkin, T. El-Raghy, *Scr. Mater.* **1997**, *36*.
[24] C. J. Rawn, M. W. Barsoum, T. El-Raghy, A. Procipio, C. M. Hoffmann, C. R. Hubbard, *Mater. Res. Bull.* **2000**, *35*, 1785–1796.
[25] B. Manoun, S. K. Saxena, T. El-Raghy, M. W. Barsoum, *Appl. Phys. Lett.* **2006**, *88*, 201902.
[26] C. Hu, J. Zhang, J. Wang, F. Li, J. Wang, Y. Zhou, *J. Am. Ceram. Soc.* **2008**, *91*, 636–639.

ChemPlusChem

Review

doi.org/10.1002/cplu.202300214

**Chemistry
Europe**
European Chemical
Societies Publishing

[27] J. Etzkorn, M. Ade, D. Kotzott, M. Kleczek, H. Hillebrecht, *J. Solid State Chem.* **2009**, *182*, 995–1002.

[28] Z. Liu, E. Wu, J. J. Wang, Y. Qian, H. Xiang, X. Li, Q. Jin, G. Sun, X. Chen, J. J. Wang, M. Li, *Acta Mater.* **2014**, *73*, 186–193.

[29] Q. Tao, M. Dahlqvist, J. Lu, S. Kota, R. Meshkian, J. Halim, J. Palisaitis, L. Hultman, M. W. Barsoum, P. O. Å Å Persson, J. Rosen, *Nat. Commun.* **2017**, *8*, 14949.

[30] B. Anasori, M. R. Lukatskaya, Y. Gogotsi, *Nat. Rev. Mater.* **2017**, *2*, 16098.

[31] S. K. Nemani, B. Zhang, B. C. Wyatt, Z. D. Hood, S. Manna, R. Khaledialidusti, W. Hong, M. G. Sternberg, S. K. R. S. Sankaranarayanan, B. Anasori, *ACS Nano* **2021**, *15*, 12815–12825.

[32] H. Ding, Y. Li, M. Li, K. Chen, K. Liang, G. Chen, J. Lu, J. Palisaitis, P. O. Å Persson, P. Eklund, L. Hultman, S. Du, Z. Chai, Y. Gogotsi, Q. Huang, *Science* **2023**, *379*, 1130–1135.

[33] M. Naguib, M. Kurtoglu, V. Presser, J. Lu, J. Niu, M. Heon, L. Hultman, Y. Gogotsi, M. W. Barsoum, *Adv. Mater.* **2011**, *23*, 4248–4253.

[34] M. Naguib, O. Mashtalir, J. Carle, V. Presser, J. Lu, L. Hultman, Y. Gogotsi, M. W. Barsoum, *ACS Nano* **2012**, *6*, 1322–1331.

[35] M. Naguib, J. Halim, J. Lu, K. M. Cook, L. Hultman, Y. Gogotsi, M. W. Barsoum, *J. Am. Chem. Soc.* **2013**, *135*, 15966–15969.

[36] X. Wang, S. Lin, H. Tong, Y. Huang, P. Tong, B. Zhao, J. Dai, C. Liang, H. Wang, X. Zhu, Y. Sun, S. Dou, *Electrochim. Acta* **2019**, *307*, 414–421.

[37] I. Persson, A. el Ghazaly, Q. Tao, J. Halim, S. Kota, V. Darakchieva, J. Palisaitis, M. W. Barsoum, J. Rosen, P. O. Å Persson, *Small* **2018**, *14*, 1703676.

[38] B. Anasori, M. Dahlqvist, J. Halim, E. J. Moon, J. Lu, B. C. Hosler, E. N. Caspi, S. J. May, L. Hultman, P. Eklund, J. Rosén, M. W. Barsoum, *J. Appl. Phys.* **2015**, *118*, 94304.

[39] M. Han, K. Maleski, C. E. Shuck, Y. Yang, J. T. Glazar, A. C. Foucher, K. Hantanasirisakul, A. Sarycheva, N. C. Frey, S. J. May, V. B. Shenoy, E. A. Stach, Y. Gogotsi, *J. Am. Chem. Soc.* **2020**, *142*, 19110–19118.

[40] G. Deysher, C. E. Shuck, K. Hantanasirisakul, N. C. Frey, A. C. Foucher, K. Maleski, A. Sarycheva, V. B. Shenoy, E. A. Stach, B. Anasori, Y. Gogotsi, *ACS Nano* **2020**, *14*, 204–217.

[41] R. Meshkian, L. Å Näslund, J. Halim, J. Lu, M. W. Barsoum, J. Rosen, *Scr. Mater.* **2015**, 147–150.

[42] J. Halim, S. Kota, M. R. Lukatskaya, M. Naguib, M. Q. Zhao, E. J. Moon, J. Pitock, J. Nanda, S. J. May, Y. Gogotsi, M. W. Barsoum, *Adv. Funct. Mater.* **2016**, *26*, 3118–3127.

[43] J. Zhou, X. Zha, X. Zhou, F. Chen, G. Gao, S. Wang, C. Shen, T. Chen, C. Zhi, P. Eklund, S. Du, J. Xue, W. Shi, Z. Chai, Q. Huang, *ACS Nano* **2017**, *11*, 3841–3850.

[44] J. Zhou, X. Zha, F. Y. Chen, Q. Ye, P. Eklund, S. Du, Q. Huang, *Angew. Chem. Int. Ed.* **2016**, *55*, 5008–5013.

[45] C. Xu, L. Wang, Z. Liu, L. Chen, J. Guo, N. Kang, X. L. Ma, H. M. Cheng, W. Ren, *Nat. Mater.* **2015**, *14*, 1135–1141.

[46] P. Urbankowski, B. Anasori, T. Makaryan, D. Er, S. Kota, P. L. Walsh, M. Zhao, V. B. Shenoy, M. W. Barsoum, Y. Gogotsi, *Nanoscale* **2016**, *8*, 11385–11391.

[47] B. Soundiraraju, B. K. George, *ACS Nano* **2017**, *11*, 8892–8900.

[48] S. Venkateshalu, J. Cherusseri, M. Karnan, K. S. Kumar, P. Kollu, M. Sathish, J. Thomas, S. K. Jeong, A. N. Grace, *ACS Omega* **2020**, *5*, 17983–17992.

[49] P. Urbankowski, B. Anasori, K. Hantanasirisakul, L. Yang, L. Zhang, B. Haines, S. J. May, S. J. L. Billinge, Y. Gogotsi, *Nanoscale* **2017**, *9*, 17722–17730.

[50] Z. Guo, J. Zhou, Z. Sun, *J. Mater. Chem. A* **2017**, *5*, 23530–23535.

[51] M. Dahlqvist, J. Rosen, *Mater Adv* **2022**, *3*, 2908–2917.

[52] B. Zhang, J. Zhou, Z. Sun, *J. Mater. Chem. A* **2022**, *10*, 15865–15880.

[53] I. Ozdemir, Y. Kadioglu, O. Üzengi Aktürk, Y. Yuksel, Ü. Akinci, E. Aktürk, *J. Phys.: Condens. Matter* **2019**, *31*, 505401.

[54] X. H. Zha, P. Xu, Q. Huang, S. Du, R. Q. Zhang, *Nanoscale Adv.* **2020**, *2*, 347–355.

[55] N. Miao, J. Wang, Y. Gong, J. Wu, H. Niu, S. Wang, K. Li, A. R. Oganov, T. Tada, H. Hosono, *Chem. Mater.* **2020**, *32*, 6947–6957.

[56] M. Dadashi Firouzjaei, M. Karimiziarani, H. Moradkhani, M. Elliott, B. Anasori, *Mater. Today* **2022**, *13*, 100202.

[57] M. Han, C. E. Shuck, R. Rakhmanov, D. Parchment, B. Anasori, C. M. Koo, G. Friedman, Y. Gogotsi, *ACS Nano* **2020**, *14*, 5008–5016.

[58] R. Khan, S. Andreescu, *Sensors* **2020**, *20*, 1–19.

[59] A. Sinha, Dhanjai, S. M. Mugo, J. Chen, K. S. Lokesh, *Handbook of Nanomaterials in Analytical Chemistry: Modern Trends in Analysis* **2020**, 361–372.

[60] P. Eklund, M. Beckers, U. Jansson, H. Högberg, L. Hultman, *Thin Solid Films* **2010**, *518*, 1851–1878.

[61] T. Rackl, L. Eisenburger, R. Niklaus, D. Johrendt, *Phys. Rev. Mater.* **2019**, *3*, 054001.

[62] Z. Li, E. Wu, K. Chen, X. Wang, G. Chen, L. Miao, Y. Zhang, Y. Song, S. Du, Z. Chai, Q. Huang, *Acta Mater.* **2022**, *237*, 118183.

[63] Z. Lin, M. Zhuo, Y. Zhou, M. Li, J. Wang, *J. Am. Ceram. Soc.* **2006**, *89*, 3765–3769.

[64] L. Zheng, J. Wang, X. Lu, F. Li, J. Wang, Y. Zhouw, *J. Am. Ceram. Soc.* **2010**, *93*, 3068–3071.

[65] C. Hu, C. C. Lai, Q. Tao, J. Lu, J. Halim, L. Sun, J. Zhang, J. Yang, B. Anasori, J. Wang, Y. Sakka, L. Hultman, P. Eklund, J. Rosen, M. W. Barsoum, *Chem. Commun.* **2015**, *51*, 6560–6563.

[66] C. C. Lai, R. Meshkian, M. Dahlqvist, J. Lu, L. Näslund, O. Rivin, E. N. Caspi, O. Ozeri, L. Hultman, P. Eklund, M. W. Barsoum, J. Rosen, *Acta Mater.* **2015**, *99*, 157–164.

[67] A. Thore, M. Dahlqvist, B. Alling, J. Rosen, *Phys. Chem. Chem. Phys.* **2016**, *18*, 12682–12688.

[68] J. Björk, J. Halim, J. Zhou, J. Rosen, *NPJ 2D Mater. Appl.* **2023**, *7*, 5.

[69] H. Fashandi, M. Dahlqvist, J. Lu, J. Palisaitis, S. I. Simak, I. A. Abrikosov, J. Rosen, L. Hultman, M. Andersson, A. Lloyd Spetz, P. Eklund, *Nat. Mater.* **2017**, *16*, 814–818.

[70] H. Zhang, D. Zhu, C. Hu, in *Advances in Ceramic Matrix Composites: Second Edition*, Elsevier Inc., **2018**, pp. 331–354.

[71] J. Zhang, B. Liu, J. Y. Wang, Y. C. Zhou, *J. Mater. Res.* **2009**, *24*, 39–49.

[72] M. Dahlqvist, J. Rosen, *Nanoscale* **2020**, *12*, 785–794.

[73] Z. Liu, L. Zheng, L. Sun, Y. Qian, J. Wang, M. Li, *J. Am. Ceram. Soc.* **2014**, *97*, 67–69.

[74] K. Hantanasirisakul, B. Anasori, S. Nemsak, J. L. Hart, J. Wu, Y. Yang, R. V. Chopdekar, P. Shafer, A. F. May, E. J. Moon, J. Zhou, Q. Zhang, M. L. Taheri, S. J. May, Y. Gogotsi, *Nanoscale Horiz.* **2020**, *5*, 1557–1565.

[75] E. N. Caspi, P. Chartier, F. Porcher, F. Damay, T. Cabioc'h, *Mater. Res. Lett.* **2015**, *3*, 100–106.

[76] B. Anasori, J. Halim, J. Lu, C. A. Voigt, L. Hultman, M. W. Barsoum, *Scr. Mater.* **2015**, *101*, 5–7.

[77] D. Gandla, F. Zhang, D. Q. Tan, *ACS Omega* **2022**, *7*, 7190–7198.

[78] R. Meshkian, Q. Tao, M. Dahlqvist, J. Lu, L. Hultman, J. Rosen, *Acta Mater.* **2017**, *125*, 476–480.

[79] M. Dahlqvist, A. Petruhins, J. Lu, L. Hultman, J. Rosen, *ACS Nano* **2018**, *12*, 7761–7770.

[80] J. Lu, A. Thore, R. Meshkian, Q. Tao, L. Hultman, J. Rosen, *Cryst. Growth Des.* **2017**, *17*, 5704–5711.

[81] R. Meshkian, M. Dahlqvist, J. Lu, B. Wickman, J. Halim, J. Thörnberg, Q. Tao, S. Li, S. Intikhab, J. Snyder, M. W. Barsoum, M. Yildizhan, J. Palisaitis, L. Hultman, P. O. Å Persson, J. Rosen, *Adv. Mater.* **2018**, *30*, 1706409.

[82] A. Petruhins, J. Lu, L. Hultman, J. Rosen, *Mater. Res. Lett.* **2019**, *7*, 446–452.

[83] A. Petruhins, M. Dahlqvist, J. Lu, L. Hultman, J. Rosen, *Cryst. Growth Des.* **2020**, *20*, 55–61.

[84] J. Thörnberg, J. Halim, J. Lu, R. Meshkian, J. Palisaitis, L. Hultman, P. O. Å Persson, J. Rosen, *Nanoscale* **2019**, *11*, 14720–14726.

[85] M. Dahlqvist, J. Lu, R. Meshkian, Q. Tao, L. Hultman, J. Rosen, *Sci. Adv.* **2017**, *3*, e1700642.

[86] L. Chen, M. Dahlqvist, T. Lapauw, B. Tunca, F. Wang, J. Lu, R. Meshkian, K. Lambrinou, B. Blanpain, J. Vleugels, J. Rosen, *Inorg. Chem.* **2018**, *57*, 6237–6244.

[87] Q. Tao, J. Lu, M. Dahlqvist, A. Mockute, S. Calder, A. Petruhins, R. Meshkian, O. Rivin, D. Potashnikov, E. N. E. N. Caspi, H. Shaked, A. Hoser, C. Opagiste, R. M. Galera, R. Salikhov, U. Wiedwald, C. Ritter, A. R. Wildes, B. Johansson, L. Hultman, M. Farle, M. W. Barsoum, J. Rosen, *Chem. Mater.* **2019**, *31*, 2476–2485.

[88] M. Dahlqvist, J. Rosen, *Nanoscale* **2022**, *14*, 10958–10971.

[89] Z. Chen, H. Chong, S. Sun, J. Yang, G. Yao, Q. Wang, J. Zhu, S. Yang, W. Cui, *Scr. Mater.* **2022**, *213*, 114596.

[90] T. Hu, Z. Li, M. Hu, J. Wang, Q. Hu, Q. Li, X. Wang, *J. Phys. Chem. C* **2017**, *121*, 19254–19261.

[91] M. Ashton, K. Mathew, R. G. Hennig, S. B. Sinnott, *J. Phys. Chem. C* **2016**, *120*, 3550–3556.

[92] T. Hu, M. Hu, B. Gao, W. Li, X. Wang, *J. Phys. Chem. C* **2018**, *122*, 18501–18509.

[93] C. Wang, H. Shou, S. Chen, S. Wei, Y. Lin, P. Zhang, Z. Liu, K. Zhu, X. Guo, X. Wu, P. M. Ajayan, L. Song, *Adv. Mater.* **2021**, *33*.

[94] M. H. Tran, F. Brilmayer, L. Liu, H. Zhuang, C. Hess, A. Andrieu-Brunsen, C. S. Birkel, *ACS Appl. Nano Mater.* **2020**, *3*, 4069–4076.

[95] K. R. G. Lim, M. Shekhirev, B. C. Wyatt, B. Anasori, Y. Gogotsi, Z. W. Seh, *Nature Synthesis* **2022**, *1*, 601–614.

[96] J. C. Schuster, H. Nowotny, *Dedicated to Prof. Dr. Konrad Schubert on his 65th birthday* **1980**, *71*, 341–346.

[97] J. C. Schuster, H. Nowotny, C. Vaccaro, *J. Solid State Chem.* **1980**, *32*, 213–219.

[98] S. Sridharan, H. Nowotny, *Int. J. Mater. Res.* **1983**, *74*, 468–472.

[99] I. Salama, T. El-Raghy, M. W. Barsoum, *J. Alloys Compd.* **2002**, *347*, 271–278.

[100] M. W. Barsoum, J. Golczewski, H. J. Seifert, F. Aldinger, *J. Alloys Compd.* **2002**, *340*, 173–179.

[101] T. Lapauw, B. Tunca, D. Potashnikov, A. Pesach, O. Ozeri, J. Vleugels, K. Lambrinou, *Sci. Rep.* **2018**, *8*, 12801.

[102] V. J. Keast, S. Harris, D. K. Smith, *Phys. Rev. B* **2009**, *80*, 214113.

[103] Y. Tan, Y. Xia, Z. Teng, C. Chen, X. Zhou, H. Zhang, *J. Eur. Ceram. Soc.* **2021**, *41*, 4658–4665.

[104] L. Chen, Y. Li, K. Chen, X. Bai, M. Li, S. Du, Z. Chai, Q. Huang, *Small Structures* **2023**, *4*, 2200161.

[105] Z. Du, C. Wu, Y. Chen, Q. Zhu, Y. Cui, H. Wang, Y. Zhang, X. Chen, J. Shang, B. Li, W. Chen, C. Liu, S. Yang, *Adv. Energy Mater.* **2022**, *12*, 2103228.

[106] N. Kubitza, R. Xie, I. Tarasov, C. Shen, H. Zhang, U. Wiedwald, C. S. Birkel, *Chem. Mater.* **2023**, *35*, 4427–4434.

[107] D. Yu, Y. Tan, *Ceram. Int.* **2021**, *47*, 30188–30193.

[108] L. Wang, Q. Chen, T. Yang, B. Guo, Y. Cheng, W. Xu, *J. Mater. Sci. Mater. Electron.* **2022**, *33*, 17446–17452.

[109] L. Qu, G. Bei, B. Stelzer, H. Rueß, J. M. Schneider, D. Cao, S. van der Zwaag, W. G. Sloof, *Ceram. Int.* **2019**, *45*, 1400–1408.

[110] M. W. Barsoum, J. Golczewski, H. J. Seifert, F. Aldinger, *J. Alloys Compd.* **2002**, *340*, 173–179.

[111] M. Naguib, M. W. Barsoum, Y. Gogotsi, *Adv. Mater.* **2021**, *33*, 2103393.

[112] A. S. Ingason, A. Mockute, M. Dahlqvist, F. Magnus, S. Olafsson, U. B. Arnalds, B. Alling, I. A. Abrikosov, B. Hjörvarsson, P. O. Å Persson, J. Rosen, *Phys. Rev. Lett.* **2013**, *110*, 195502.

[113] A. S. Ingason, A. Petruhins, M. Dahlqvist, F. Magnus, A. Mockute, B. Alling, L. Hultman, I. A. Abrikosov, P. O. Å Persson, J. Rosen, *Mater. Res. Lett.* **2013**, *2*, 89–93.

[114] J. M. Schneider, Z. Sun, R. Mertens, F. Uestel, R. Ahuja, *Solid State Commun.* **2004**, *130*, 445–449.

[115] M. Dahlqvist, B. Alling, J. Rosen, *J. Phys. Condens. Matter* **2015**, *27*, 095601.

[116] M. Jaouen, M. Bugnet, N. Jaouen, P. Ohresser, V. Mauchamp, T. Cabioc'h, A. Rogalev, *J. Phys. Condens. Matter* **2014**, *26*, 176002.

[117] A. Petruhins, A. S. Ingason, J. Lu, F. Magnus, S. Olafsson, J. Rosen, *J. Mater. Sci.* **2015**, *50*, 4495–4502.

[118] R. Salikhov, A. S. Semisalova, A. Petruhins, A. S. Ingason, J. Rosen, U. Wiedwald, M. Farle, *Mater. Res. Lett.* **2015**, *3*, 156–160.

[119] M. Magnuson, M. Mattesini, *J. Magn. Magn. Mater.* **2020**, *501*, 166470.

[120] A. Mockute, P. O. Å Persson, F. Magnus, A. S. Ingason, S. Olafsson, L. Hultman, J. Rosen, *Phys. Status Solidi RRL* **2014**, *8*, 420–423.

[121] A. Petruhins, B. Arni Sigurdur Ingason, B. Jun Lu, B. Fridrik Magnus, B. Sveinn Olafsson, B. Johanna Rosen, *J. Mater. Sci.* **2015**, *50*, 4495–4502.

[122] A. Mockute, J. Lu, E. J. Moon, M. Yan, B. Anasori, S. J. May, M. W. Barsoum, J. Rosen, *Mater. Res. Lett.* **2015**, *3*, 16–22.

[123] Z. Liu, T. Waki, Y. Tabata, H. Nakamura, *Phys. Rev. B* **2014**, *89*, 54435.

[124] C. M. Hamm, J. D. Bocarsly, G. Seward, U. I. Kramm, C. S. Birkel, *J. Mater. Chem. C* **2017**, *5*, 5700–5708.

[125] K. Sobolev, H. Pazniak, M. Farle, V. Rodionova, U. Wiedwald, *J. Mater. Chem. C* **2021**, *9*, 16516–16522.

[126] J. P. Siebert, S. Mallett, M. Juelsholt, H. Pazniak, U. Wiedwald, K. Page De, C. S. Birkel, K. Page, C. S. Birkel, *Mater. Chem. Front.* **2021**, *5*, 6082–6091.

[127] Q. Tao, R. Salikhov, A. Mockute, J. Lu, M. Farle, U. Wiedwald, J. Rosen, *APL Mater.* **2016**, *4*, 86109.

[128] D. Ohmer, I. Opahle, H. K. Singh, H. Zhang, *J. Phys. Condens. Matter* **2019**, *31*, 405902.

[129] W. Jeitschko, H. Nowotny, F. Benesovsky, *Monatsh. Chem.* **1963**, *94*, 1198–1200.

[130] M. W. Barsoum, L. Farber, I. Levin, A. Procopio, T. El-Raghy, A. Berner, *J. Am. Ceram. Soc.* **1999**, *82*, 2545–2547.

[131] H. Nowotny, *Prog. Solid State Chem.* **1971**, *5*, 27–70.

[132] W. Jeitschko, I. L. Nowotny, F. Benesovsky, H. Nowotny, F. Benesovsky, *Monatsh. Chem.* **1964**, *95*, 178–179.

[133] D. T. Cuskelly, E. R. Richards, E. H. Kisi, V. J. Keast, *J. Solid State Chem.* **2015**, *230*, 418–425.

[134] J. P. Palmquist, S. Li, P. O. Å Persson, J. Emmerlich, O. Wilhelmsson, H. Högberg, M. I. Katsnelson, B. Johansson, R. Ahuja, O. Eriksson, L. Hultman, U. Jansson, *Phys. Rev. B: Condens. Matter Mater. Phys.* **2004**, *70*, 1–13.

[135] Q. Tao, M. Dahlqvist, J. Lu, S. Kota, R. Meshkian, J. Halim, J. Palisaitis, L. Hultman, M. W. Barsoum, P. O. Å Persson, J. Rosen, *Nat. Commun.* **2017**, *8*, 14949.

[136] D. Horlait, S. Grasso, A. Chroneos, W. E. Lee, *Mater. Res. Lett.* **2016**, *4*, 137–144.

[137] G. P. Bei, V. Gauthier-Brunet, C. Tromas, S. Dubois, *J. Am. Ceram. Soc.* **2012**, *95*, 102–107.

[138] J. Etzkorn, M. Ade, H. Hillebrecht, *Inorg. Chem.* **2007**, *46*, 1410–1418.

[139] T. Cabioch, P. Eklund, V. Mauchamp, M. Jaouen, M. W. Barsoum, *J. Eur. Ceram. Soc.* **2013**, *33*, 897–904.

[140] E. Zapata-Solvas, S. R. G. Christopoulos, N. Ni, D. C. Parfitt, D. Horlait, M. E. Fitzpatrick, A. Chroneos, W. E. Lee, *J. Am. Ceram. Soc.* **2017**, *100*, 1377–1387.

[141] W. Yu, S. Li, W. G. Sloof, *Mater. Sci. Eng. A* **2010**, *527*, 5997–6001.

[142] S. Wo, Z. Huang, L. Cai, W. Hu, Y. Wang, Y. Zhou, H. Zhai, *Int. J. Appl. Ceram. Technol.* **2019**, *16*, 2398–2408.

[143] A. Ganguly, T. Zhen, M. W. Barsoum, *J. Alloys Compd.* **2004**, *376*, 287–295.

[144] L. Cai, Z. Huang, W. Hu, C. Lei, S. Wo, X. Li, H. Zhai, Y. Zhou, *Ceram. Int.* **2018**, *44*, 9593–9600.

[145] T. Lapauw, B. Tunca, D. Potashnikov, A. Pesach, O. Ozeri, J. Vleugels, K. Lambrinou, *Sci. Rep.* **2018**, *8*, 12801.

[146] B. Tunca, T. Lapauw, R. Delville, D. R. Neuville, L. Hennet, D. Thiaudière, T. Ouisse, J. Hadermann, J. Vleugels, K. Lambrinou, *Inorg. Chem.* **2019**, *58*, 6669–6683.

[147] B. Tunca, G. Greaves, J. A. Hinks, P. O. Å Persson, J. Vleugels, K. Lambrinou, *Acta Mater.* **2021**, *206*, 116606.

[148] H. Boller, H. Nowotny, *Monatsh. Chem.* **1966**, *97*, 1053–1058.

[149] H. Boller, H. Nowotny, *Monatsh. Chem.* **1968**, *99*, 672–675.

[150] O. Beckmann, H. Boller, H. Nowotny, F. Benesovsky, *Monatsh. Chem.* **1969**, *100*, 1465–1470.

[151] J. Sinclair, J. P. Siebert, M. Juelsholt, C. Shen, H. Zhang, C. S. Birkel, *Inorg. Chem.* **2022**, *61*, 16976–16980.

[152] O. Beckmann, H. Boller, H. Nowotny, *Monatsh. Chem.* **1968**, *99*, 1580–1583.

[153] X. Wang, K. Chen, E. Wu, Y. Zhang, H. Ding, N. Qiu, Y. Song, S. Du, Z. Chai, Q. Huang, *J. Eur. Ceram. Soc.* **2022**, *42*, 2084–2088.

[154] K. Chen, X. Bai, X. Mu, P. Yan, N. Qiu, Y. Li, J. Zhou, Y. Song, Y. Zhang, S. Du, Z. Chai, Q. Huang, *J. Eur. Ceram. Soc.* **2021**, *41*, 4447–4451.

[155] M. Li, J. Lu, K. Luo, Y. Li, K. Chang, K. Chen, J. Zhou, J. Rosen, L. Hultman, P. Eklund, P. O. Å Persson, S. Du, Z. Chai, Z. Huang, Q. Huang, *J. Am. Chem. Soc.* **2019**, *141*, 4730–4737.

[156] H. Ding, Y. Li, J. Lu, K. Luo, K. Chen, M. Li, P. O. Å Persson, L. Hultman, P. Eklund, S. Du, Z. Huang, Z. Chai, H. Wang, P. Huang, Q. Huang, *Mater. Res. Lett.* **2019**, *7*, 510–516.

[157] Y. Li, J. Liang, H. Ding, J. Lu, X. Mu, P. Yan, X. Zhang, K. Chen, M. Li, P. O. Å Persson, L. Hultman, P. Eklund, S. Du, H. Yang, Z. Chai, Q. Huang, *Appl. Phys.* **2021**, *8*, DOI 10.1063/5.0059078.

[158] M. Nechiche, T. Cabioc'H, E. N. Caspi, O. Rivin, A. Hoser, V. Gauthier-Brunet, P. Chartier, S. Dubois, *Inorg. Chem.* **2017**, *56*, 14388–14395.

[159] Y. Li, M. Li, J. Lu, B. Ma, Z. Wang, L. Z. Cheong, K. Luo, X. Zha, K. Chen, P. O. Å Persson, L. Hultman, P. Eklund, C. Shen, Q. Wang, J. Xue, S. Du, Z. Huang, Z. Chai, Q. Huang, *ACS Nano* **2019**, *13*, 9198–9205.

[160] M. Nechiche, V. Gauthier-Brunet, V. Mauchamp, A. Joulain, T. Cabioc'h, X. Milhet, P. Chartier, S. Dubois, *J. Eur. Ceram. Soc.* **2017**, *37*, 459–466.

[161] C. C. Lai, H. Fashandi, J. Lu, J. Palisaitis, P. O. Å Persson, L. Hultman, P. Eklund, J. Rosen, *Nanoscale* **2017**, *9*, 17681–17687.

[162] Y. Li, J. Liang, H. Ding, J. Lu, X. Mu, P. Yan, X. Zhang, K. Chen, M. Li, P. O. Å Persson, L. Hultman, P. Eklund, S. Du, H. Yang, Z. Chai, Q. Huang, *Appl. Phys.* **2021**, *8*, 031418.

[163] C. C. Lai, A. Petruhins, J. Lu, M. Farle, L. Hultman, P. Eklund, J. Rosen, *Mater. Res. Lett.* **2017**, *5*, 533–539.

[164] A. L. Greenaway, C. L. Melamed, M. B. Tellekamp, R. Woods-Robinson, E. S. Toberer, J. R. Neilson, A. C. Tamboli, *Annu. Rev. Mater. Res.* **2020**, *51*, 1–28.

[165] J. M. D. Coey, P. A. I. Smith, *J. Magn. Magn. Mater.* **1999**, *200*, 405–424.

[166] T. Joelsson, A. Hörling, J. Birch, L. Hultman, *Appl. Phys. Lett.* **2005**, *86*, 111913.

[167] T. Scabarozi, A. Ganguly, J. D. Hettinger, S. E. Lofland, S. Amini, P. Finkel, T. El-Raghy, M. W. Barsoum, *J. Appl. Phys.* **2008**, *104*, 73713.

[168] Z. J. Lin, M. J. Zhuo, M. S. Li, J. Y. Wang, Y. C. Zhou, *Scr. Mater.* **2007**, *56*, 1115–1118.

[169] M. W. Barsoum, M. Ali, T. El-Raghy, *Metall. Mater. Trans. A* **2000**, *31*, 1857–1865.

[170] Y. Liu, L. L. Zhang, W. Xiao, L. L. Zhang, Y. Pu, S. Guo, *Mater. Lett.* **2015**, *149*, 5–7.

[171] L. Gröner, L. Mengis, M. Galetz, L. Kirste, P. Daum, M. Wirth, F. Meyer, A. Fromm, B. Blug, F. Burmeister, *Materials* **2020**, *13*, 2085.

[172] B. Keskin, S. A. Naziri Mehrabani, S. Arefi-Oskoui, V. Vatanpour, O. Orhun Teber, A. Khataee, Y. Orooji, I. Koyuncu, *Carbohydr. Polym.* **2022**, *296*, 119913.

[173] Z. Liu, T. Waki, Y. Tabata, K. Yuge, H. Nakamura, I. Watanabe, *Phys. Rev. B: Condens. Matter Mater. Phys.* **2013**, *88*, 1–7.

[174] H. Tong, S. Lin, Y. Huang, P. Tong, W. Song, Y. Sun, *Intermetallics* **2019**, *105*, 39–43.

[175] Y. Li, J. Liu, W. Liu, X. Zhu, H. H. Wen, *Philos. Mag.* **2015**, *95*, 2831–2837.

[176] A. D. Bortolozo, G. Serrano, A. Serquis, D. Rodrigues, C. A. M. Dos Santos, Z. Fisk, A. J. S. MacHado, *Solid State Commun.* **2010**, *150*, 1364–1366.

[177] W. Jeitschko, H. Nowotny, F. Benesovsky, *Monatsh. Chem.* **1964**, *95*, 156–157.

[178] N. Kubitza, A. Reitz, A.-M. Zieschang, H. Pazniak, B. Albert, C. Kalha, C. Schlueter, A. Regoutz, U. Wiedwald, C. S. Birkel, *Inorg. Chem.* **2022**, *61*, 10634–10641.

[179] M. A. Pietzka, J. C. Schuster, *J. Am. Ceram. Soc.* **1996**, *79*, 2321–2330.

[180] T. Cabioc'h, P. Eklund, V. Mauchamp, M. Jaouen, *J. Eur. Ceram. Soc.* **2012**, *32*, 1803–1811.

[181] S. Kota, M. Sokol, M. W. Barsoum, *Int. Mater. Rev.* **2020**, *65*, 226–255.

[182] W. Jeitschko, *Monatsh. Chem.* **1966**, *97*, 1472–1476.

[183] Y. B. Kuz'ma, N. Chaban, *Izv. Akad. Nauk SSSR Neorg. Mater.* **1969**, *5*, 384–385.

[184] G. B. Carpenter, *Acta Crystallogr.* **1969**, *B25*, 163.

[185] N. F. Chaban, Y. B. Kuz'ma, *Neorg. Mater.* **1973**, *9*, 1908–1911.

[186] H. Zhang, F. zhi Dai, H. Xiang, Z. Zhang, Y. Zhou, *J. Mater. Sci. Technol.* **2019**, *35*, 530–534.

[187] M. Ade, H. Hillebrecht, *Inorg. Chem.* **2015**, *54*, 6122–6135.

[188] W. Jung, K. Petry, *Z. Kristallogr.* **1988**, *18*, 153–154.

[189] W. Jung, K. Schweitzer, *Z. Kristallogr.* **1986**, *174*, 109–110.

[190] S. Hirt, F. Hilfinger, H. Hillebrecht, *Z. Kristallogr.* **2018**, *233*, 295–307.

[191] C. Shen, Q. Gao, N. M. Fortunato, H. K. Singh, I. Opahle, O. Gutfleisch, H. Zhang, *J. Mater. Chem. A* **2021**, *9*, 8805–8813.

[192] Y. Zhou, H. Xiang, F. Z. Dai, Z. Feng, *J. Mater. Sci. Technol.* **2018**, *34*, 1441–1448.

[193] J. Wang, T. N. Ye, Y. Gong, J. Wu, N. Miao, T. Tada, H. Hosono, *Nat. Commun.* **2019**, *10*, 2284.

[194] Y. Zhou, H. Xiang, F. Z. Dai, Z. Feng, *J. Am. Ceram. Soc.* **2018**, *101*, 2459–2470.

[195] M. Dahlqvist, J. Rosen, Q. Tao, J. Zhou, J. Palisaitis, P. O. Å Persson, *J. Am. Chem. Soc.* **2020**, *142*, 18583–18591.

[196] Q. Tao, J. Palisaitis, Y. Li, Q. Huang, P. O. Å Persson, J. Rosen, *Mater. Res. Lett.* **2022**, *10*, 295–300.

[197] Q. Du, G. Chen, W. Yang, J. Wei, M. Hua, H. Du, C. Wang, S. Liu, J. Han, Y. Zhang, J. Yang, *J. Phys. D* **2015**, *48*, 335001.

[198] S. Hirt, F. Yuan, Y. Mozharivskyj, H. Hillebrecht, *Inorg. Chem.* **2016**, *55*, 9677–9684.

[199] L. A. Hanner, H. O. Badr, M. Dahlqvist, S. Kota, D. Raczkowski, J. Rosen, M. W. Barsoum, *Mater. Res. Lett.* **2021**, *9*, 112–118.

[200] D. Potashnikov, E. N. Caspi, A. Pesach, A. Hoser, S. Kota, L. Verger, M. W. Barsoum, I. Felner, A. Keren, O. Rivin, *J. Magn. Magn. Mater.* **2019**, *471*, 468–474.

[201] K. Kádas, D. Iuşan, J. Hellsvik, J. Cedervall, P. Berastegui, M. Sahlberg, U. Jansson, O. Eriksson, *J. Phys. Condens. Matter* **2017**, *29*, 155402.

[202] X. Tan, P. Chai, C. M. Thompson, M. Shatruk, *J. Am. Chem. Soc.* **2013**, *135*, 9553–9557.

[203] M. ElMassalami, D. da S Oliveira, H. Takeya, *J. Magn. Magn. Mater.* **2011**, *323*, 2133–2136.

[204] V. Franco, J. S. Blázquez, B. Ingale, A. Conde, *Annu. Rev. Mater. Res.* **2012**, *42*, 305–342.

[205] M. Dahlqvist, J. Zhou, I. Persson, B. Ahmed, J. Lu, J. Halim, Q. Tao, J. Palisaitis, J. Thörnberg, P. Helmer, L. Hultman, P. O. Å Persson, J. Rosen, *Adv. Mater.* **2021**, *142*, 18583–18591.

[206] T. A. ElMeligy, S. Kota, V. Natu, H. Lind, J. Palisaitis, P. O. Å Persson, J. Rosen, M. W. Barsoum, *J. Alloys Compd.* **2021**, *888*, 161377.

[207] M. Werwiński, S. Kontos, K. Gunnarsson, P. Svedlindh, J. Cedervall, V. Höglin, M. Sahlberg, A. Edström, O. Eriksson, J. Rusz, *Phys. Rev. B* **2016**, *93*, 174412.

[208] L. H. Iggstrijm, R. Wappling, Y. Andersson, S. Rundqvist, *J. Solid State Chem.* **1975**, *13*, 84–91.

[209] M. A. McGuire, D. S. Parker, *J. Appl. Phys.* **2015**, *118*, 16.

[210] S. Rundqvist, *Acta Chem. Scand.* **1962**, *16*, 1–19.

[211] C. Bormio-Nunes, C. A. Nunes, A. A. Coelho, M. I. S. T. Faria, P. A. Suzuki, G. C. Coelho, *J. Alloys Compd.* **2010**, *508*, 5–8.

[212] Z. G. Xie, D. Y. Geng, Z. D. Zhang, *Appl. Phys. Lett.* **2010**, *97*, 202504.

[213] J. Zhou, J. Palisaitis, J. Halim, M. Dahlqvist, Q. Tao, I. Persson, L. Hultman, P. O. Å Persson, J. Rosen, *Science* **2021**, *373*, 801–805.

[214] H. Zhang, H. Xiang, F. zhi Dai, Z. Zhang, Y. Zhou, *J. Mater. Sci. Technol.* **2018**, *34*, 2022–2026.

[215] L. T. Alameda, R. W. Lord, J. A. Barr, P. Moradifar, Z. P. Metzger, B. C. Steimle, C. F. Holder, N. Alem, S. B. Sinnott, R. E. Schaak, *J. Am. Chem. Soc.* **2019**, *141*, 10852–10861.

[216] K. Kim, C. Chen, D. Nishio-Hamane, M. Okubo, A. Yamada, *Chem. Commun.* **2019**, *55*, 9295–9298.

[217] L. T. Alameda, P. Moradifar, Z. P. Metzger, N. Alem, R. E. Schaak, *J. Am. Chem. Soc.* **2018**, *140*, 8833–8840.

[218] H. Zhang, F. Z. Dai, H. Xiang, X. Wang, Z. Zhang, Y. Zhou, *J. Mater. Sci. Technol.* **2019**, *35*, 1593–1600.

[219] L. T. Alameda, C. F. Holder, J. L. Fenton, R. E. Schaak, *Chem. Mater.* **2017**, *29*, 8953–8957.

[220] M. Dou, H. Li, Q. Yao, J. Wang, Y. Liu, F. Wu, *Phys. Chem. Chem. Phys.* **2021**, *23*, 10615–10620.

[221] X. Liu, X. Ge, Y. Dong, K. Fu, F. Meng, R. Si, M. Zhang, X. Xu, *Mater. Chem. Phys.* **2020**, *253*, 12334.

[222] B. Zhang, J. Zhou, Z. Guo, Q. Peng, Z. Sun, *Appl. Surf. Sci.* **2020**, *500*, 144248.

[223] Z. Jiang, P. Wang, X. Jiang, J. Zhao, *Nanoscale Horiz.* **2018**, *3*, 335–341.

[224] I. Ozdemir, Y. Kadioglu, Y. Yüksel, Ü. Aklncl, O. Ü. Aktürk, E. Aktürk, S. Ciraci, *Phys. Rev. B* **2021**, *103*, 144424.

[225] D. P. Riley, E. H. Kisi, *J. Am. Ceram. Soc.* **2007**, *90*, 2231–2235.

[226] C. Hu, Z. Lin, L. He, Y. Bao, J. Wang, M. Li, Y. Zhou, *J. Am. Ceram. Soc.* **2007**, *90*, 2542–2548.

[227] H. Högberg, L. Hultman, J. Emmerlich, T. Joelsson, P. Eklund, J. M. Molina-Aldareguia, J.-P. Palmquist, O. Wilhelmsson, U. Jansson, *Surf. Coat. Technol.* **2005**, *193*, 6–10.

[228] O. Wilhelmsson, J.-P. Palmquist, E. Lewin, J. Emmerlich, P. Eklund, P. O. Å Persson, H. Högberg, S. Li, R. Ahuja, O. Eriksson, *J. Cryst. Growth* **2006**, *291*, 290–300.

[229] P. Eklund, A. Murugaiah, J. Emmerlich, Z. Czigány, J. Frodelius, M. W. Barsoum, H. Högberg, L. Hultman, *J. Cryst. Growth* **2007**, *304*, 264–269.

[230] H. Högberg, J. Emmerlich, P. Eklund, O. Wilhelmsson, J. P. Palmquist, U. Jansson, L. Hultman, in *Advances in Science and Technology*, Trans Tech Publ, **2006**, pp. 2648–2655.

[231] W. Jeitschko, H. Nowotny, F. Benesovsky, *Monatsh. Chem.* **1963**, *94*, 672–676.

[232] T. Lapauw, J. Halim, J. Lu, T. Cabioc'h, L. Hultman, M. W. Barsoum, K. Lambrinou, J. Vleugels, *J. Eur. Ceram. Soc.* **2016**, *36*, 943–947.

[233] T. Lapauw, K. Lambrinou, T. Cabioc'h, J. Halim, J. Lu, A. Pesach, O. Rivin, O. Ozeri, E. N. Caspi, L. Hultman, *J. Eur. Ceram. Soc.* **2016**, *36*, 1847–1853.

[234] B. Tunca, T. Lapauw, O. M. Karakulina, M. Batuk, T. Cabioc'h, J. Hadermann, R. Delville, K. Lambrinou, J. Vleugels, *Inorg. Chem.* **2017**, *56*, 3489–3498.

[235] Y. Li, P. Bai, *Int. J. Refract. Met. Hard Mater.* **2011**, *29*, 751–754.

[236] D. P. Riley, E. H. Kisi, T. C. Hansen, A. W. Hewat, *J. Am. Ceram. Soc.* **2002**, *85*, 2417–2424.

[237] D. P. Riley, E. H. Kisi, D. Phelan, *J. Eur. Ceram. Soc.* **2006**, *26*, 1051–1058.

[238] D. P. Riley, E. H. Kisi, T. C. Hansen, *J. Am. Ceram. Soc.* **2008**, *91*, 3207–3210.

[239] A. Sedghi, R. Vahed, *Iran. J. Mater. Sci. Eng.* **2014**, *2*.

[240] A. Zhou, C.-A. Wang, Z. Ge, L. Wu, *J. Mater. Sci. Lett.* **2001**, *20*, 1971–1973.

[241] M. Akhlaghi, S. A. Tayebifard, E. Salahi, M. S. Asl, G. Schmidt, *Ceram. Int.* **2018**, *44*, 9671–9678.

[242] M. J. Abu, J. J. Mohamed, Z. A. Ahmad, *Int. Scholarly Res. Not.* **2012**, *2012*, 341285 .

[243] A. Dash, R. Vaßen, O. Guillon, J. Gonzalez-Julian, *Nat. Mater.* **2019**, *18*, 465–470.

[244] C. Roy, P. Banerjee, S. Bhattacharyya, *J. Eur. Ceram. Soc.* **2020**, *40*, 923–929.

[245] C. Giordano, C. Erpen, W. Yao, M. Antonietti, *Nano Lett.* **2008**, *8*, 4659–4663.

[246] J. P. Siebert, L. Bischoff, M. Lepple, A. Zintler, L. Molina-Luna, U. Wiedwald, C. S. Birkel, *J. Mater. Chem. C* **2019**, *7*, 6034–6040.

[247] J. P. Siebert, K. Patarakun, C. S. Birkel, *Inorg. Chem.* **2022**, *61*, 1603–1610.

[248] J. P. Siebert, M. Juelsholt, D. Günzing, H. Wende, K. Ollefs, C. S. Birkel, *Inorg. Chem. Front.* **2022**, *9*, 1565–1574.

[249] J. P. Siebert, M. Flores, C. S. Birkel, *ACS Org. Inorg. Au* **2022**, *2*, 59–65.

[250] J. P. Siebert, D. Hajra, S. Tongay, C. S. Birkel, *Nanoscale* **2022**, *14*, 744–751.

[251] J. P. Siebert, C. M. Hamm, C. S. Birkel, *Appl. Phys.* **2019**, *6*, 41314.

[252] W. T. Sutton, *Am. Ceram. Soc. Bull.* **1989**, *68*, 376–386.

[253] D. K. Agrawal, *Curr. Opin. Solid State Mater. Sci.* **1998**, *3*, 480–485.

[254] H. J. Kitchen, S. R. Vallance, J. L. Kennedy, N. Tapia-Ruiz, L. Carassiti, A. Harrison, A. G. Whittaker, T. D. Drysdale, S. W. Kingman, D. H. Gregory, *Chem. Rev.* **2014**, *114*, 1170–1206.

[255] C. M. Hamm, T. Schäfer, H. Zhang, C. S. Birkel, *Ceram. Int.* **2016**, 1397–1401.

[256] C. M. Hamm, M. Dürrschnabel, L. Molina-Luna, R. Salikhov, D. Spoddig, M. Farle, U. Wiedwald, C. S. Birkel, *Mater. Chem. Front.* **2018**, *2*, 483–490.

[257] N. C. Ghosh, S. P. Harimkar, in *Advances in Science and Technology of $M_{n+1}AX_n$ Phases* (Ed.: I. M. Low), Woodhead Publishing, **2012**, pp. 47–80.

[258] Z. A. Munir, U. Anselmi-Tamburini, M. Ohyanagi, *J. Mater. Sci.* **2006**, *41*, 763–777.

[259] J. Zhang, L. Wang, W. Jiang, L. Chen, *J. Alloys Compd.* **2007**, *437*, 203–207.

[260] W. Tian, K. Vanmeensel, P. Wang, G. Zhang, Y. Li, J. Vleugels, O. Van der Biest, *Mater. Lett.* **2007**, *61*, 4442–4445.

[261] N. Goossens, T. Lapauw, K. Lambrinou, J. Vleugels, *J. Eur. Ceram. Soc.* **2022**, *42*, 7389–7402.

[262] M. Anayee, N. Kurra, M. Alhabeb, M. Seredych, M. N. Hedhili, A. H. Emwas, H. N. Alshareef, B. Anasori, Y. Gogotsi, *Chem. Commun.* **2020**, *56*, 6090–6093.

[263] M. Alhabeb, K. Maleski, B. Anasori, P. Lelyukh, L. Clark, S. Sin, Y. Gogotsi, *Chem. Mater.* **2017**, *29*, 7633–7644.

[264] F. Shahzad, M. Alhabeb, C. B. Hatter, B. Anasori, S. M. Hong, C. M. Koo, Y. Gogotsi, *Science* **2016**, *353*, 1137–1140.

[265] F. Liu, A. Zhou, J. Chen, J. Jia, W. Zhou, L. Wang, Q. Hu, *Appl. Surf. Sci.* **2017**, *416*, 781–789.

[266] M. Wu, B. Wang, Q. Hu, L. Wang, A. Zhou, *Materials* **2018**, *11*, 8–11.

[267] A. Feng, Y. Yu, F. Jiang, Y. Wang, L. Mi, Y. Yu, L. Song, *Ceram. Int.* **2017**, *43*, 6322–6328.

[268] R. Meshkian, L. Å Näslund, J. Halim, J. Lu, M. W. Barsoum, J. Rosen, *Scr. Mater.* **2015**, *108*, 147–150.

[269] J. Halim, S. Kota, M. R. Lukatskaya, M. Naguib, M. Q. Zhao, E. J. Moon, J. Pitock, J. Nanda, S. J. May, Y. Gogotsi, M. W. Barsoum, *Adv. Funct. Mater.* **2016**, *26*, 3118–3127.

[270] T. Hu, S. Zhu, Z. Li, D. Li, H. Liu, C. Zhang, X. Wang, *Unveiling the Spontaneous Conversion of Layered MAX Phases to 2D MXenes* **2022**, arXiv preprint arXiv:2208.03000.

[271] M. Khazaei, M. Arai, T. Sasaki, C. Y. Chung, N. S. Venkataramanan, M. Estili, Y. Sakka, Y. Kawazoe, *Adv. Funct. Mater.* **2013**, *23*, 2185–2192.

[272] M. H. Tran, A. M. Malik, M. Dürrschnabel, A. Regoutz, P. Thakur, T. L. Lee, D. Perera, L. Molina-Luna, K. Albe, J. Rohrer, C. S. Birkel, *Dalton Trans.* **2020**, *49*, 12215–12221.

[273] S. Y. Pang, Y. T. Wong, S. Yuan, Y. Liu, M. K. Tsang, Z. Yang, H. Huang, W. T. Wong, J. Hao, *J. Am. Chem. Soc.* **2019**, *141*, 9610–9616.

[274] B. Soundiraraju, R. Raghavan, B. K. George, *ACS Appl. Nano Mater.* **2020**, *3*, 11007–11016.

[275] O. Akinola, I. Chakraborty, H. Celio, D. Akinwande, J. A. C. Incorvia, *J. Mater. Res.* **2021**, *36*, 1980–1989.

[276] M. Hai Tran, *Exfolierbarkeit Diverser Übergangsmetallbasierter MAX-Phasen* **2021**, Dissertation.

[277] R. Khaledialidusti, M. Khazaei, S. Khazaei, K. Ohno, *Nanoscale* **2021**, *13*, 7294–7307.

[278] B. Anasori, Y. Xie, M. Beidaghi, J. Lu, B. C. Hosler, L. Hultman, P. R. C. Kent, Y. Gogotsi, M. W. Barsoum, *ACS Nano* **2015**, *9*, 9507–9516.

[279] J. Yang, X. Zhou, X. Luo, S. Zhang, L. Chen, *Appl. Phys. Lett.* **2016**, *109*, DOI 10.1063/1.4967983.

[280] Y. Li, H. Shao, Z. Lin, J. Lu, L. Liu, B. Duployer, P. O. Å Persson, P. Eklund, L. Hultman, M. Li, K. Chen, X. H. Zha, S. Du, P. Rozier, Z. Chai, E. Raymundo-Piñero, P. L. Taberna, P. Simon, Q. Huang, *Nat. Mater.* **2020**, *19*, 894–899.

[281] H. Dong, P. Xiao, N. Jin, B. Wang, Y. Liu, Z. Lin, *ChemElectroChem* **2021**, *8*, 957–962.

[282] L. Y. Xiu, Z. Y. Wang, J. S. Qiu, *Rare Met.* **2020**, *39*, 1237–1238.

[283] L. Liu, M. Orbay, S. Luo, S. Duluard, H. Shao, J. Harmel, P. Rozier, P. L. Taberna, P. Simon, *ACS Nano* **2022**, *16*, 111–118.

[284] W. Sun, S. A. Shah, Y. Chen, Z. Tan, H. Gao, T. Habib, M. Radovic, M. J. Green, *J. Mater. Chem. A* **2017**, *5*, 21663–21668.

[285] S. Yang, P. Zhang, F. Wang, A. G. Ricciardulli, M. R. Lohe, P. W. M. Blom, X. Feng, *Angew. Chem. Int. Ed.* **2018**, *57*, 15491–15495.

[286] T. Li, L. Yao, Q. Liu, J. Gu, R. Luo, J. Li, X. Yan, W. Wang, P. Liu, B. Chen, W. Zhang, W. Abbas, R. Naz, D. Zhang, *Angew. Chem. Int. Ed.* **2018**, *57*, 6115–6119.

[287] H. Shi, P. Zhang, Z. Liu, S. W. Park, M. R. Lohe, Y. Wu, A. Shaygan Nia, S. Yang, X. Feng, *Angew. Chem. Int. Ed.* **2021**, *60*, 8689–8693.

[288] R. A. Vaia, A. Jawaid, A. Hassan, G. Neher, D. Nepal, R. Pachter, W. Joshua Kennedy, S. Ramakrishnan, *ACS Nano* **2021**, *15*, 2771–2777.

[289] J. Mei, G. A. Ayoko, C. Hu, J. M. Bell, Z. Sun, *Sustainable Mater. Technol.* **2020**, *25*, e00156.

[290] J. Mei, G. A. Ayoko, C. Hu, Z. Sun, *Chem. Eng. J.* **2020**, *395*,125111.

[291] A. El Ghazaly, H. Ahmed, A. R. Rezk, J. Halim, P. O. Å Persson, L. Y. Yeo, J. Rosen, *ACS Nano* **2021**, *15*, 4287–4293.

[292] S. Zada, W. Dai, Z. Kai, H. Lu, X. Meng, Y. Zhang, Y. Cheng, F. Yan, P. Fu, X. Zhang, H. Dong, *Angew. Chem.* **2020**, *132*, 6663–6668.